# Asymmetrical Organic D-π-A Conjugate with *'V'*-Shape Crystal Packing: Quest to Transcend the Limits of Photophysical Properties and Applications

Shouvik Bhuin[1], Purbali Chakraborty[2], Pandiyan Sivasakthi[3], Pralok K Samanta[3], Perumal Yogeeswari[2], Manab Chakravarty[1]*

[1]Department of Chemistry, [2]Department of Pharmacy, BITS-Pilani Hyderabad Campus, Hyderabad-500078, India; [3]Department of Chemistry, School of Science, Gandhi Institute for Technology and Management (GITAM), Hyderabad-502329, India


| Topics | Page No |
|---|---|
| Scheme S1. Synthetic pathway to prepare (*E*)-1-hexyl-3-(10-(4-(pyridin-2-yl)styryl)anthracen-9-yl)-1H-indole *(IAPY)* | 4 |
| Materials and Methods | 5-7 |
| **Fig. S1** Different planes of **IAPY** | 8 |
| **Fig. S2** single-crystal with the dihedral angles in three different twisted sites | 8 |
| **Fig. S3** '*V*'-shaped herringbone packing of **IAPY** | 8 |
| **Fig. S4** Label atom for **IAPY** | 9 |
| **Table S1** Short-contacts | 9 |
| **Fig. S5** Rotational and screw-axes of **IAPY** | 10 |
| **Fig. S6** Glide plains in packing of **IAPY** | 10 |
| **Fig. S7** Contact surface void of **IAPY** | 11 |
| **Fig. S8a** Solid-state (a) absorbances (b) emission and MIEE properties of **IAPY** | 11 |
| **Fig. S8b** Photostability of **IAPY** pristine | 11 |
| **Fig. S9** Software generated dendrogram for **IAPY** pristine | 12 |
| **Table S2** Peak list for **IAPY** pristine PXRD | 12 |
| **Fig. S10** Software generated dendrogram for **IAPY** ground | 13 |
| **Table S3** Peak list for **IAPY** ground PXRD | 13 |
| **Fig. S11** Surface accessible void of **IAPY** | 14 |
| **Fig. S12** DSC for the 3rd time ground form of **IAPY** | 14 |
| **Fig. S13** Hirshfeld surface of **IAPY** | 14 |

| | |
|---|---|
| **Fig. S14** Hirshfeld surface and van dar Waals and the non-covalent interactions to the packing for **IAPY** | 15 |
| **Table S4** Inter-molecular potentials | 15-16 |
| **Fig. S15** Decay profile of **IAPY** for MIEE property | 16 |
| **Fig. S16** SEM images for **IAPY** (a) pristine (b) ground (c) recovered | 16 |
| **Fig. S17** Absorbances for **IAPY** SSAC | 17 |
| **Fig. S18a** Changes in PXRD pattern for **IAPY** due to acidofluorochromism | 17 |
| **Fig. S18b** SEM images for **IAPY** (a) acid-fumed (b) base-fumed | 18 |
| **Fig. S19** Decay profile for **IAPY** (a) acid-fumed (**IAPYH**) (b) base-fumed | 18 |
| **Fig. S20** DSC for the '4$^{th}$ day post to base treatment' form of **IAPY** | 18 |
| **Fig. S21** Absorbances of **IAPY** in different solvents | 19 |
| **Fig. S22** TD-DFT optimized structures and calculations for **IAPY** in Hexane and N,N-DMF | 19 |
| **Fig. S23a** CV experimental plots for HOMO-LUMO for **IAPY** in Hexane and N,N-DMF, the procedure and the calculation | 19-20 |
| **Fig. S23b** HOMO-LUMO for **IAPY** in Hexane and N,N-DMF using CAM-B3LYP/6-31G* | 21 |
| **Fig. S23c** HOMO-LUMO for **IAPY** in Hexane and N,N-DMF using PBE0/6-31G* level of theory | 21 |
| **Fig. S23d** NTOs for **IAPY** in Hexane and N,N-DMF using CAM-B3LYP/6-31G* | 22 |
| **Fig. S23e** Hole and electron NTOs in the $S_1$ state of **IAPY** in DCM and DMF solvent with PBE0/6-31G* level of theory | 22 |
| **Table S5** Calculation of Electronic Properties in DFT and DCM Solvent | 23 |
| **Table S6** Optimized Ground State ($S_0$) Geometry in DCM solvent | 23-24 |
| **Table S7** Optimized Ground State ($S_0$) Geometry in DMF solvent | 24 |
| **Table S8** DSE properties of **IAPY** | 25 |
| **Fig. S24** HOMO-LUMO for **IAPY** in Hexane and N,N-DMF | 25 |
| **Fig. S25** Dihedral scanning for emission oscillator strength at different twisted sites of **IAPY** | 25 |

| | |
|---|---|
| **Fig. S26** Decay profiles of **IAPY** in different solvents | 26 |
| **Fig. S27** LE state emissions of **IAPY** in different solvents | 26 |
| **Fig. S28** CIE-coordinates of whitish emission of **IAPY** | 27 |
| **Fig. S29a** Absorbances for whitish emission for **IAPY** in the binary mixture of 1,4-dioxane and $CHCl_3$ | 27 |
| **Fig. S29b** Whitish emission for **IAPY** in the binary mixture of 1,4-dioxane and $CHCl_3$ | 28 |
| **Fig. S30** Whitish emission for **IAPY** in the binary mixture of EtOAc and $CHCl_3$ | 28 |
| **Table S9** Results of times-resolved studies | 29 |
| **Fig. S31** Absorbances for AIE-study of **IAPY** | 30 |
| **Fig. S32** Intensity of emission increment for AIE at $10^{-5}$M concentration of **IAPY**<br>**Fig. S33** TD-DFT optimized structure of **IAPY** in water | 30<br>31 |
| **Fig. S34a** Rotation barrier of the Pyridine group in $S_1$ state | 31 |
| **Fig. S34b** TD-DFT optimized structure of **IAPY** in MeOH | 32 |
| **Fig. S35** Absorbances for viscofluorochromism of **IAPY** | 32 |
| **Fig. S36** Intensity of emission increment for VIE at $10^{-5}$M concentration of **IAPY** | 33 |
| **Fig. S37** Cellular uptake of the probe **IAPY** through Fluorescence Activated Cell Sorting (FACS) | 33 |
| **Fig. S38** Bright field images for wash-free bioimaging of FaDu with **IAPY** | 34 |
| Cell culture and confocal microscopy | 34 |
| FACS | 34 |
| Device fabrication, formulation with dye for screen printing and the procedure for screen printing | 34-35 |
| Procedure and method of data storage and anticounterfeiting applications with stimuli-responsive hidden stamp | 35 |

| | |
|---|---|
| **Fig. S39** Data encryption with **IAPY** | 35 |
| **Fig. S40** Data encryption with **IAPY** to make different digits from '8' | 36 |
| **Fig. S41** Xanthan gum sensing | 36 |
| **Fig. S42** Na-CMC sensing | 37 |
| **Fig. S43** False-positive taste | 37 |
| **Fig. S44a** Blood serum NMR | 38 |
| **Fig. S44b** Blood serum-NMR comparison | 38 |
| **Fig. S45** Hospital-disposed of biohazards detection by fluorescence | 39 |
| **Fig. S46** $^{1}$H NMR of **IAPY** | 39 |
| **Fig. S47** $^{1}$H NMR of **IAPYH** | 40 |
| **Fig. S48** $^{13}$C NMR of **IAPY** | 40 |
| **Fig. S49a** $^{13}$C NMR of **IAPYH** | 41 |
| **Fig. S49b** $^{13}$C NMR (aromatic part zoomed) of **IAPYH** | 41 |
| References | 42 |


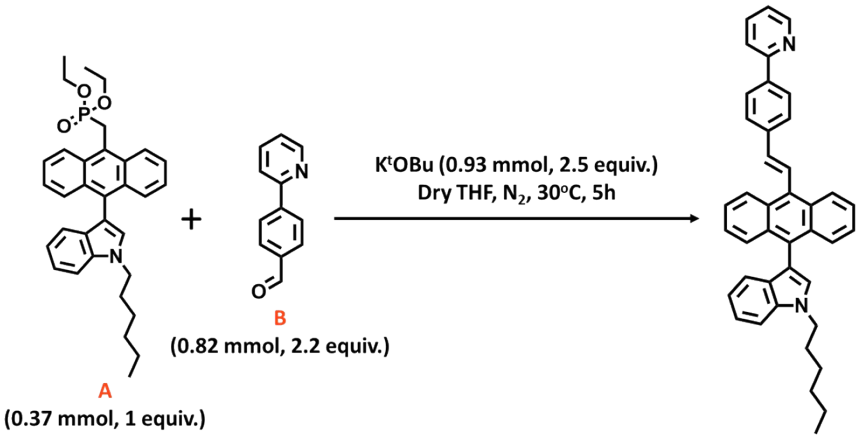


**Scheme S1.** Synthetic pathway to prepare **(*E*)-1-hexyl-3-(10-(4-(pyridin-2-yl)styryl)anthracen-9-yl)-1H-indole *(IAPY)***[1]

**Synthetic procedure and characterization of IAPY[1]**

Diethyl ((10-(1-hexyl-1H-indol-3yl)anthracen-9-yl)methyl)phosphonate (0.37 mmol, 1 equiv., 0.2 g), 4-(pyridin-2-yl)benzaldehyde (0.82 mmol, 2.2 equiv., 0.15 g) and $K^tOBu$ base (0.93 mmol, 2.5 equiv., 0.1 g) were taken in a two-neck round bottom flask and allowed for vacuum drying for 5 min. Later, $N_2$ was purged throughout the flask and kept sealed with a silicon septum. An $N_2$-containing balloon was placed at one end, and at the other neck, dry THF (15 mL) was injected into the flask to stir for 5 h. The progress of the reaction was observed by eluting TLC into hexane/ EtOAc (12% EtOAc into hexane (v/v)) medium to see an intense green fluorescent product spot formed at $R_f$ = 0.29. The reaction mixture was then worked up with 30 mL of an EtOAc and brine water mixture of 1:2 EtOAc:$H_2O$. The organic layer was separated, passed through a $Na_2SO_4$ layer, finally to prepare a slurry with silica gel (60–120 mesh) for performing column chromatography (10% EtOAc into hexane (v/v)), which yielded (71%, 0.15 g) product which is a solid yellowish compound under room light but a bright yellowish-green fluorescent compound under a UV-365 nm bulb. NMR spectroscopy: $^1$H NMR (400 MHz, $CDCl_3$, 25 $^o$C, $\delta$): 8.74 (s, 1H), 8.46 (d, *J* = 8.76 Hz, 2H), 8.13–7.93 (m, 5H), 7.82–7.75 (m, 4H), 7.53–7.43 (m, 3H), 7.32–7.23 (m, 5H), 7.14–7.01 (m, 3H), 4.30 (t, *J* = 7.04 Hz, 2H), 1.99 (quint, *J* = 7.32 Hz, 2H), 1.46–1.23 (m, 6H), 0.90 (t, *J* = 7.04 Hz, 3H). $^{13}$C NMR: (100 MHz, $CDCl_3$,25$^o$C, $\delta$): 156.9, 149.8, 138.8, 138.1, 136.9, 136.1, 132.4, 131.6, 130.2, 129.8, 129.7, 128.9, 127.9, 127.3, 127.2, 127.0, 126.2, 126.1, 125.3, 124.9, 122.2, 121.8, 120.6, 120.5, 119.5, 111.9, 109.6, 46.6, 31.5, 30.3, 26.8, 22.6, 14.0. IR (KBr, $cm^{-1}$): 3445, 3048, 2944, 2849, 1580, 1467, 1431, 1345, 1322, 1233, 1147, 1017, 958. M.p.: 154–156$^0$C. Mass spectrometry: HRMS (ESI) m/z: calcd for $C_{41}H_{36}N_2$ 556.2878, found: 557.2674 $[M + H]^+$.

## Materials and Methods

### Steady-state absorption and fluorescence measurements

Solid-state absorption spectra were recorded u sing a JASCO-500 spectrophotometer, and the solution-state absorption spectra were recorded using a UV-vis-NIR spectrophotometer (Hitachi F7000, Japan). Solution-state emission spectra were obtained using an FP-6300 spectrometer (JASCO), and by using a 10 mm path-length quartz cuvette, while the solid-state emission spectra were received using a fluorimeter (Fluorolog, HORIBA). All the emission spectra were obtained at the corresponding absorption wavelengths.

Absolute/relative quantum yield and time-resolved lifetime decay measurement

The absolute quantum yield ($\Phi_f$) values for solid samples were measured using the calibrated integrating sphere method with a fluorimeter (Fluorolog, HORIBA), and absolute errors within ~± 2% have been included while for the relative quantum yield (relative $\Phi_f$) in the solution state, the error is ±5%.

Time-resolved fluorescence measurements were measured using a time-correlated single-photon counting (TCSPC) unit (Horiba Deltaflex). The laser used for all the samples was of 510 nm. All the measurements were undergone at room temperature. The decay fitting was done by keeping the $\chi^2$ value close to 1.

The average lifetime was obtained by fitting the decay profiles to a tri- or bi-exponential function eqn-1. Fit = A1.exp (-t/ τ1) + A2.exp (-t/ τ2) + A3.exp (-t/ τ3) ……..……(eq-1) α1, α 2 are the weighted components and τ1, τ2, τ3 are the individual lifetime components of the decay. The qualities of the fit were understood by judging the chi square (χ2) values. The rate constants are calculated by using: $k_r = [\Phi_f / \tau_{avg}]\ s^{-1}$; $k_{nr} = [1-\Phi_f / \tau_{avg}]\ s^{-1}$

Powder X-ray diffraction and IR spectra

The PXRD spectra of the pristine, ground, and recovered forms of the compound **IAPY** were recorded by using a Rigaku Ultima IV X-ray diffractometer, and keeping the parameters constant for all samples, with a step width of 0.21 and a scan rate of 21 min1 from 5–501 (Cu Kα radiation, l = 1.54 Å). And an FT-IR spectrometer (FT/IR-4200, Jasco) was utilized to record the IR spectra of the samples. Solid samples were mixed with KBr to form pellets to record the spectra.

Calculation of crystallinity from PXRD

Crystallinity is considered as the ratio between the area of crystalline peaks to the area of all peaks. Here the crystallinity is revealed as a percentage just by multiplying the ratio with 100. The decovolution of the PXRD raw data was completed using oringin lab software (Origin Pro 8.5, student version) having a good increment of peaks. Then by selecting the plot the 'Analysis' menu should be clicked followed by the 'Peaks and Baseline' and 'Peak Analyzer' to reach to the 'Open Dialogue'. Here, the 'Peak Analyzer Window' will be opened to perform 'Integrate Peaks.' Followed by the 'Next' option, the 'Constant Y' should be selected to well set up the baseline. Again, 'Next' and 'Find'

options should be clicked and 'Untick' to 'Enable Auto Find' should be done. Next 'Add' option should be clicked and all the relevant peaks should be selected accordingly. Next, the 'Done' option should be clicked. In the 'Peak Finding Setting' the 'Direction' should be selected as 'Positive' and 'Next' button should be clicked again. Here 'Adjust ad Preview Graph' should be done. Next the 'Finish' button has to be clicked. Now, from the grown window, 'Select Data' then 'Select Integral Results' should be copied and pasted in a new excel sheet. It was named as 'Area of crystalline peaks'. Here sum it in excel. The area will be obtained. Therefore, the same process should be undergone again but this time not specific peaks but the 'Total area' should have to be integrated and the total area thus can be calculated using the excel sheet. Finally, the area under relevant crystalline peaks should be divided by the total area under the PXRD signal and multiplied by 100 to get the percentage of crystallinity.[2]

### Differential scanning calorimetry analysis

DSC thermograms were recorded by using a Themys One$^{+}$ (Setaram) instrument keeping the temperature in the range of 30–300 °C with a ramp rate of 2 °C $min^{-1}$ under a $N_2$ atmosphere.

### Density functional theory studies

All the density functional theoretical (DFT) calculations were undergone using the ORCA Version 5.0.3 quantum chemical software package.[3,4] Our DFT calculations were done using different DFT functionals (viz., CAM-B3LYP, PBE0, B3LYP, WB97X, BHandHLYP and M06-2X) and 6-31G* basis set to compare with experimental results.[5] The excited stats ($S_1$) geometry optimization was done using time-dependent DFT (TDDFT). Root mean square deviation (RMSD) calculations were performed using the Kabsch algorithm.[6] All structural and MOs were made visualized using Avogadro software.[7]

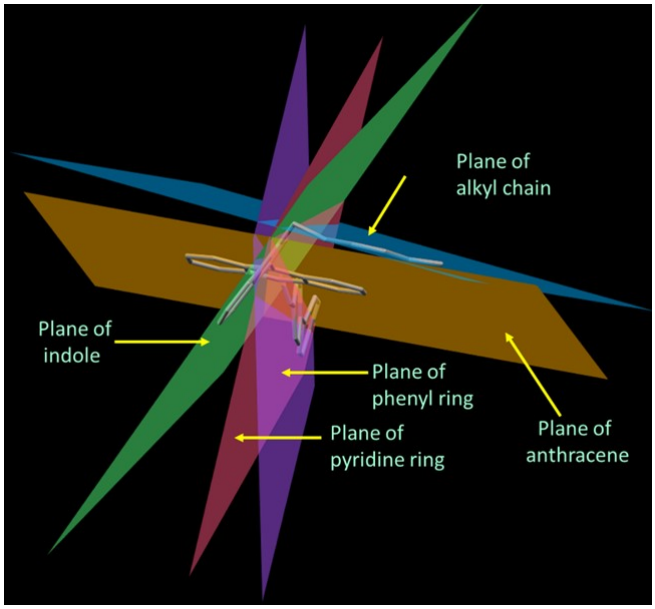


**Fig. S1** Different planes of **IAPY**

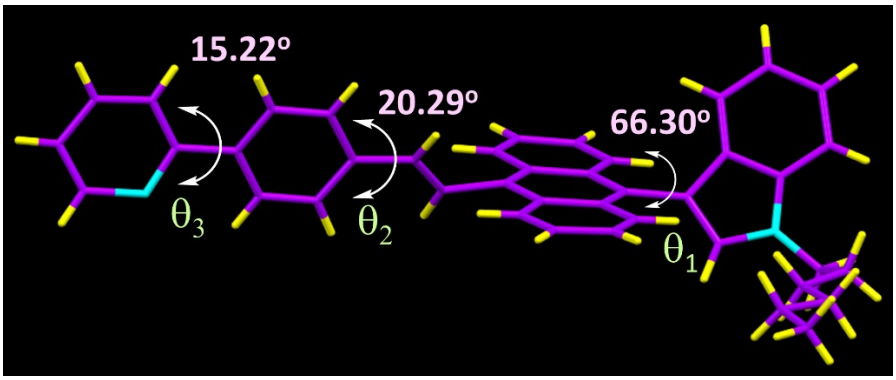


**Fig. S2** single-crystal with the dihedral angles in three different twisted sites

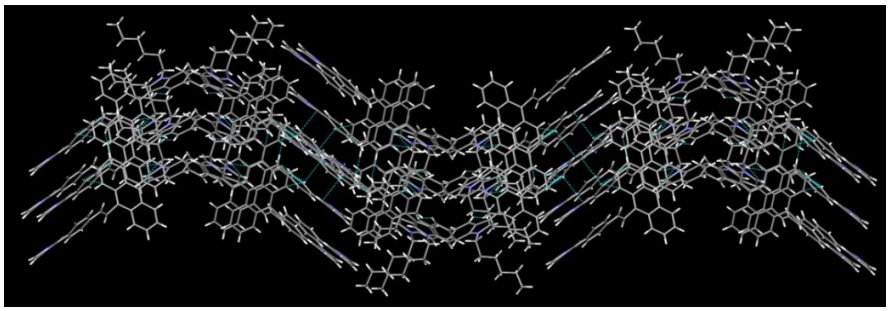

**Fig. S3** '*V*'-shaped herringbone packing of **IAPY**

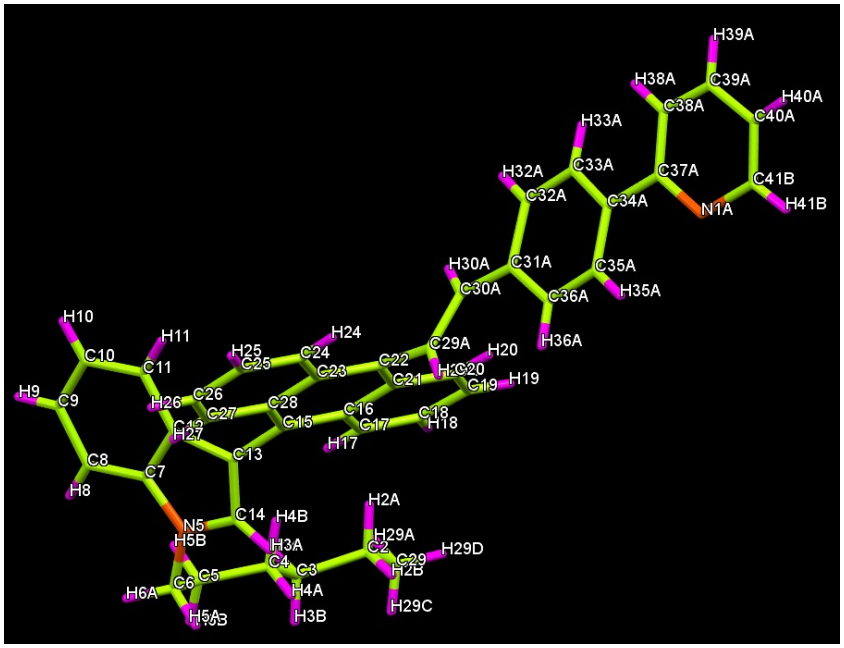


**Fig. S4** Label atom for **IAPY**

**Table S1** Short-contacts

| No | Atom1 | Atom2 | Length (A) |
|---|---|---|---|
| 1 | C13 | H27 | 2.60 |
| 2 | C13 | H17 | 2.55 |
| 3 | C12 | C27 | 3.34 |
| 4 | C12 | H27 | 2.76 |
| 5 | N1A | H35A | 2.48 |
| 6 | C14 | C17 | 3.22 |
| 7 | C14 | H17 | 2.64 |
| 8 | C14 | C4 | 3.33 |
| 9 | C8 | H6A | 2.89 |
| 10 | C24 | H29E | 2.89 |
| 11 | H24 | C29A | 2.46 |
| 12 | C20 | C30A | 3.22 |
| 13 | H20 | C30A | 2.63 |
| 14 | H20 | C29A | 2.72 |
| 15 | C38A | H33A | 2.57 |
| 16 | H38A | C33A | 2.55 |
| 17 | H38A | H33A | 1.97 |
| 18 | H3B | H29C | 2.36 |
| 19 | H30A | H32A | 2.37 |
| 20 | C36A | H29E | 2.86 |
| 21 | H36A | C29A | 2.85 |
| 22 | H36A | H29E | 2.39 |

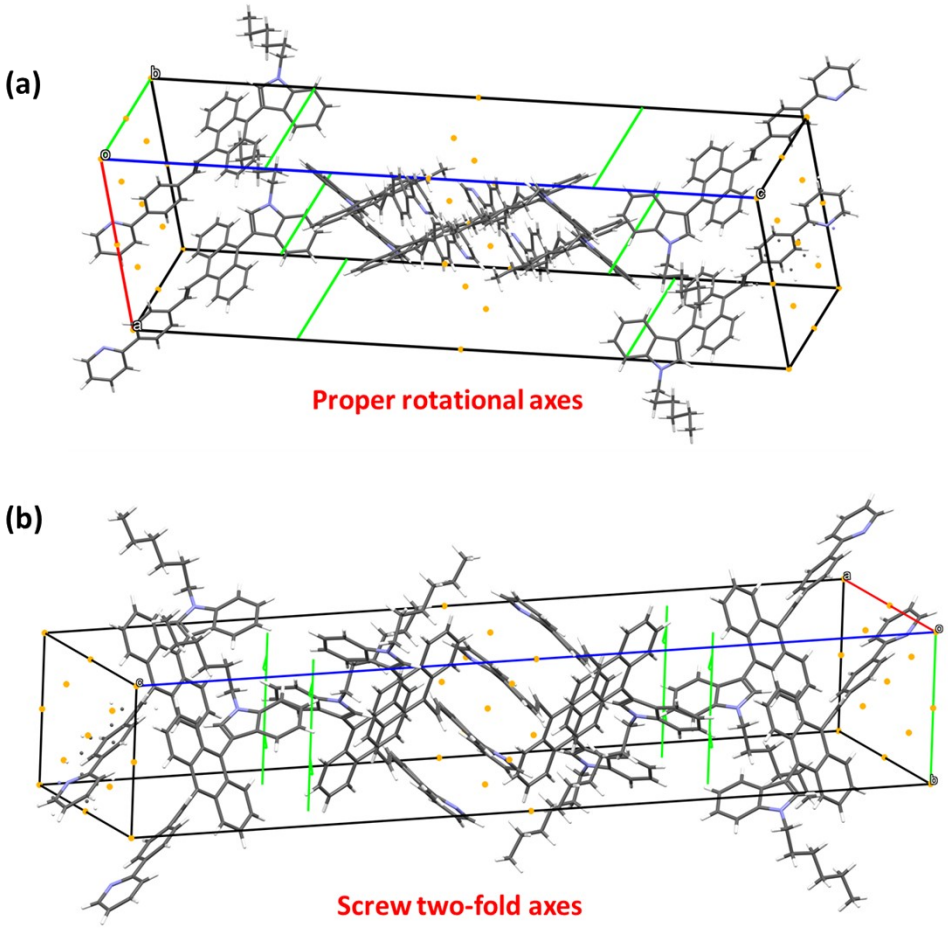


**Fig. S5** Rotational and screw-axes of **IAPY**

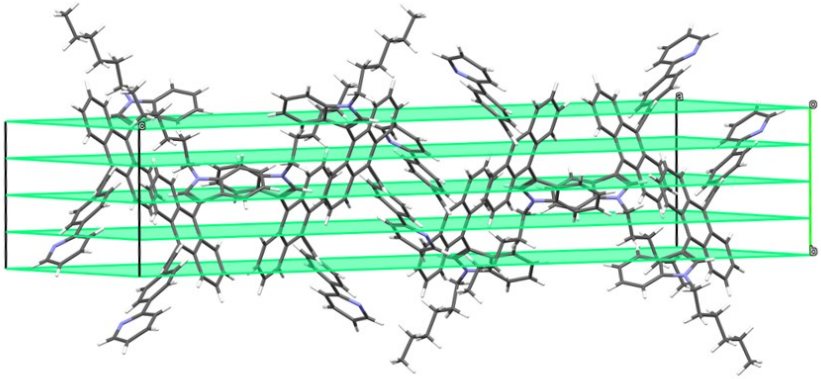

**Fig. S6** Glide plains in packing of **IAPY**

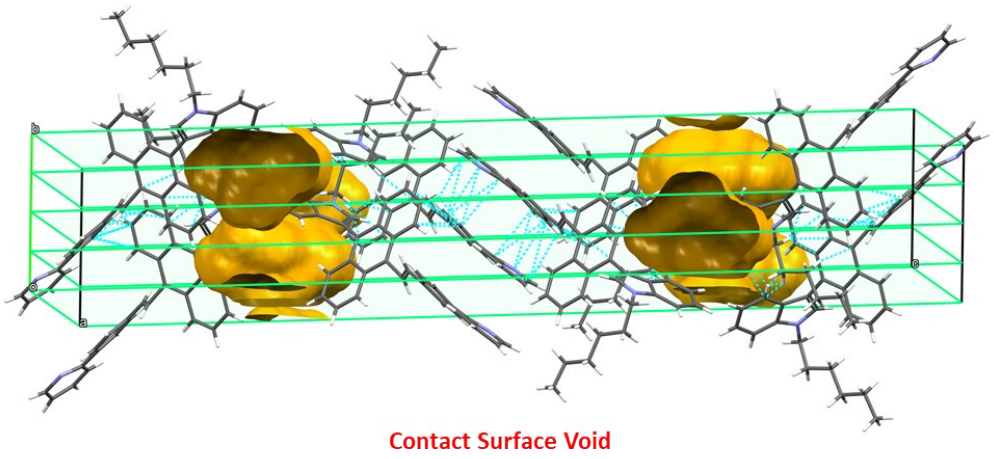


**Fig. S7** Contact surface void of **IAPY**

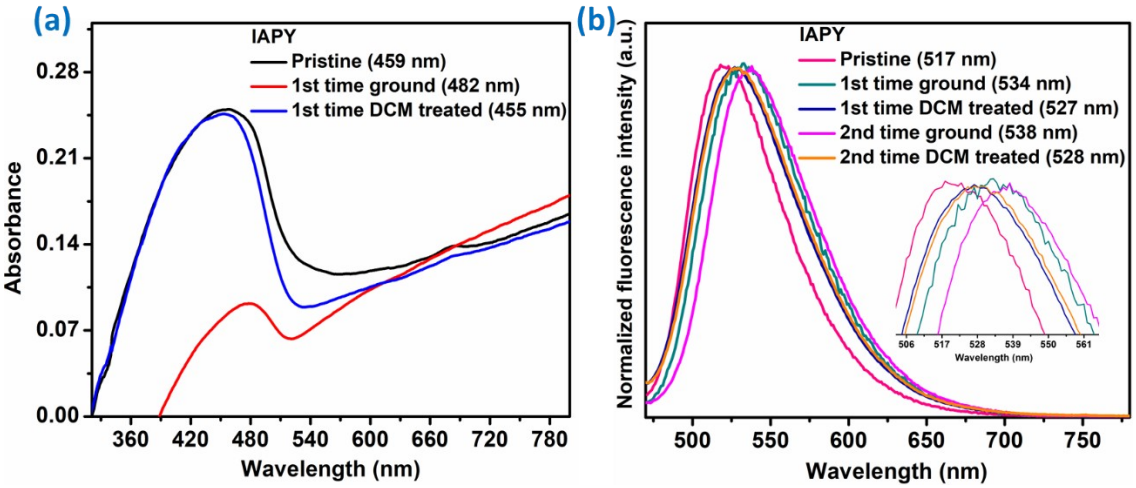


**Fig. S8a** Solid-state (a) absorbances (b) emission and MIEE properties of **IAPY**

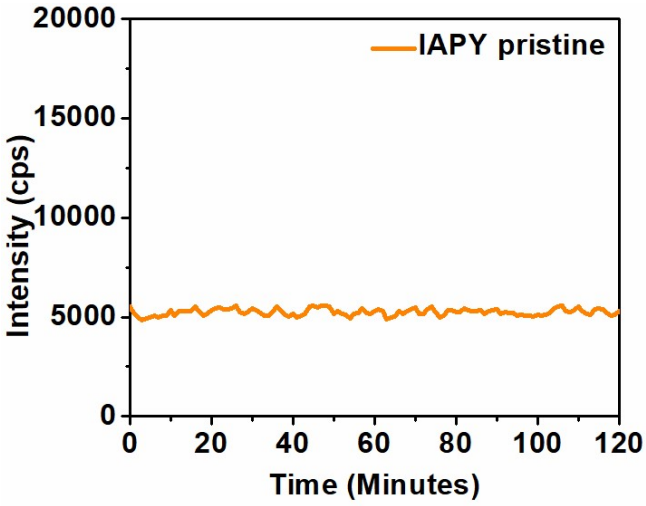


**Fig. S8b** Photostability of **IAPY** pristine

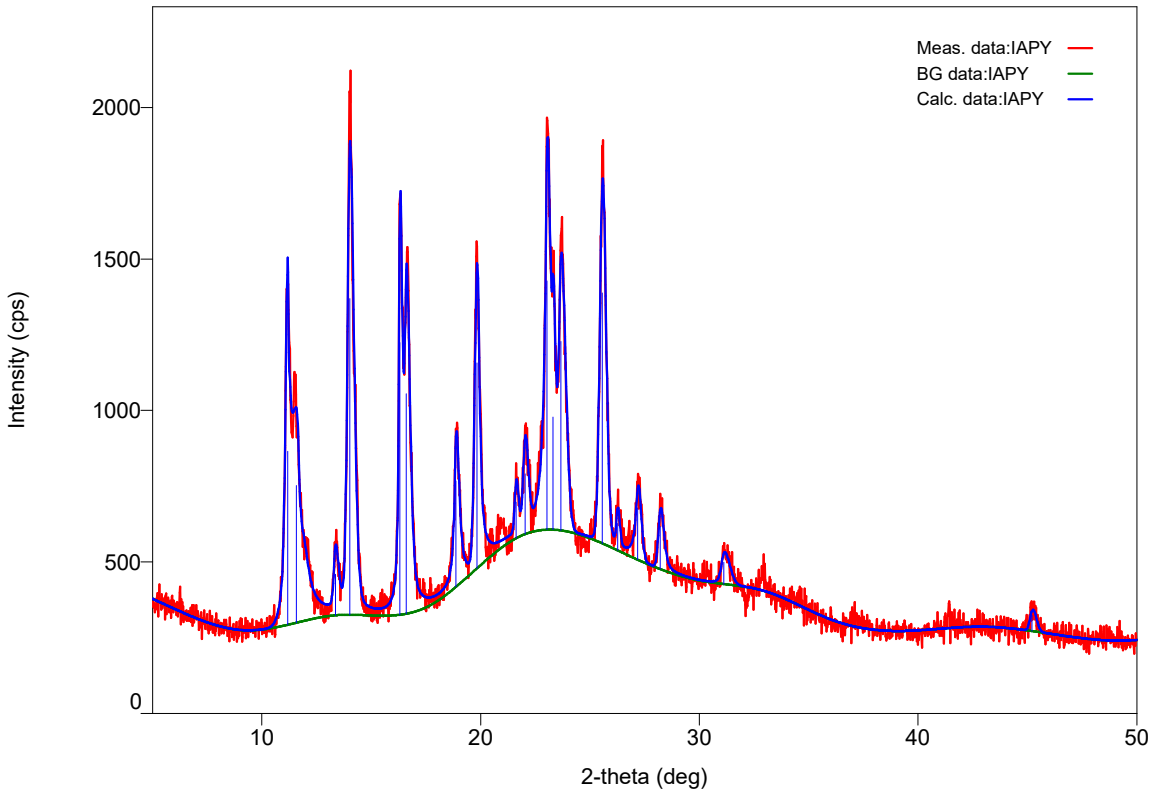


**Fig. S9** Software generated dendrogram for **IAPY** pristine

**Table S2** Peak list for **IAPY** pristine PXRD

| No. | 2-theta(deg) | d(ang.) | Height(cps) | FWHM(deg) | Int. I(cps deg) | Int. W(deg) | Asym. factor |
|---|---|---|---|---|---|---|---|
| 1 | 11.182(5) | 7.907(3) | 573(24) | 0.166(10) | 133(11) | 0.23(3) | 2.2(2) |
| 2 | 11.584(13) | 7.633(8) | 453(21) | 0.64(2) | 404(11) | 0.89(7) | 2.2(2) |
| 3 | 13.366(10) | 6.619(5) | 135(12) | 0.26(3) | 41(4) | 0.30(6) | 0.58(6) |
| 4 | 14.016(2) | 6.3136(11) | 1044(32) | 0.342(7) | 420(8) | 0.40(2) | 0.58(6) |
| 5 | 16.309(6) | 5.430(2) | 899(30) | 0.177(11) | 217(13) | 0.24(2) | 0.53(11) |
| 6 | 16.606(8) | 5.334(3) | 727(27) | 0.291(15) | 288(14) | 0.40(3) | 0.53(11) |
| 7 | 18.881(5) | 4.6962(11) | 349(19) | 0.254(18) | 134(5) | 0.38(3) | 0.6(2) |
| 8 | 19.836(3) | 4.4723(7) | 678(26) | 0.255(9) | 221(6) | 0.33(2) | 1.1(2) |
| 9 | 21.62(2) | 4.106(4) | 120(11) | 0.20(5) | 26(4) | 0.22(6) | 0.7(4) |
| 10 | 22.03(3) | 4.031(6) | 199(14) | 0.26(3) | 57(7) | 0.29(6) | 0.7(4) |
| 11 | 23.028(7) | 3.8591(12) | 821(29) | 0.26(2) | 285(19) | 0.35(3) | 0.61(9) |
| 12 | 23.309(12) | 3.8132(19) | 372(19) | 0.16(2) | 79(13) | 0.21(5) | 0.61(9) |
| 13 | 23.665(12) | 3.7565(18) | 624(25) | 0.382(17) | 323(13) | 0.52(4) | 0.61(9) |
| 14 | 25.567(8) | 3.4813(11) | 827(29) | 0.325(7) | 306(7) | 0.37(2) | 0.87(9) |
| 15 | 26.267(14) | 3.3901(17) | 89(9) | 0.17(4) | 17(3) | 0.19(5) | 0.87(9) |
| 16 | 27.186(8) | 3.2775(10) | 170(13) | 0.28(2) | 63(4) | 0.37(5) | 0.8(4) |
| 17 | 28.22(3) | 3.160(3) | 140(12) | 0.29(3) | 51(4) | 0.36(6) | 0.7(3) |
| 18 | 31.12(2) | 2.872(2) | 72(8) | 0.44(6) | 36(6) | 0.50(14) | 0.5(4) |
| 19 | 45.21(9) | 2.004(4) | 52(7) | 0.31(6) | 17(4) | 0.33(12) | 0.7(8) |

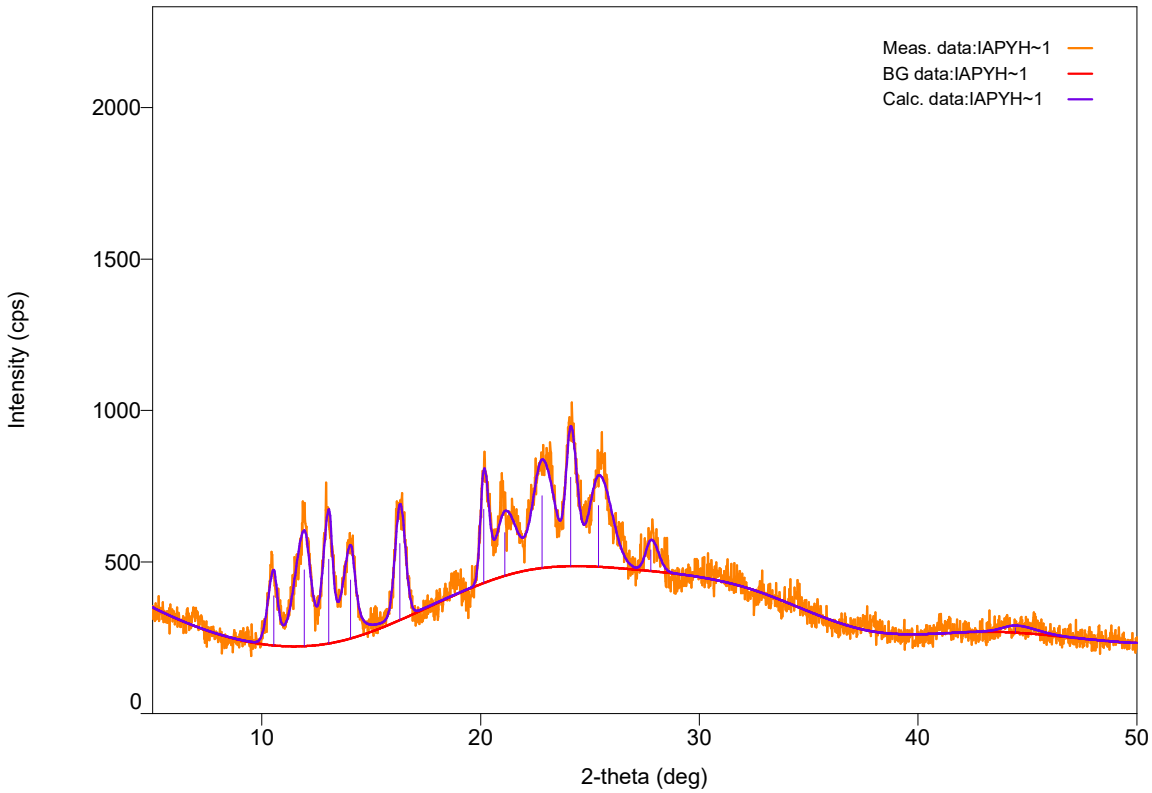


**Fig. S10** Software generated dendrogram for **IAPY** ground

**Table S3** Peak list for **IAPY** ground PXRD

| No. | 2-theta(deg) | d(ang.) | Height(cps) | FWHM(deg) | Int. I(cps deg) | Int. W(deg) | Asym. factor |
|---|---|---|---|---|---|---|---|
| 1 | 10.540(14) | 8.387(11) | 165(13) | 0.52(3) | 104(5) | 0.63(8) | 1.48(15) |
| 2 | 11.94(2) | 7.405(13) | 252(16) | 0.84(3) | 260(7) | 1.03(9) | 1.48(15) |
| 3 | 13.062(12) | 6.773(6) | 278(17) | 0.488(19) | 167(5) | 0.60(5) | 1.48(15) |
| 4 | 14.057(17) | 6.295(8) | 193(14) | 0.62(4) | 148(7) | 0.77(9) | 1.48(15) |
| 5 | 16.309(7) | 5.431(2) | 253(16) | 0.546(18) | 152(6) | 0.60(6) | 0.96(15) |
| 6 | 20.145(13) | 4.404(3) | 244(16) | 0.43(2) | 111(8) | 0.46(6) | 0.78(9) |
| 7 | 21.12(3) | 4.204(6) | 142(12) | 1.12(9) | 170(10) | 1.19(17) | 0.78(9) |
| 8 | 22.81(3) | 3.896(5) | 238(15) | 1.15(5) | 291(11) | 1.22(12) | 0.78(9) |
| 9 | 24.113(13) | 3.688(2) | 294(17) | 0.57(2) | 180(8) | 0.61(6) | 0.78(9) |
| 10 | 25.40(3) | 3.504(4) | 202(14) | 1.21(6) | 261(9) | 1.29(14) | 0.78(9) |
| 11 | 27.79(3) | 3.208(4) | 69(8) | 0.67(8) | 50(5) | 0.72(16) | 0.78(9) |
| 12 | 44.45(13) | 2.037(6) | 16(4) | 1.8(4) | 30(9) | 1.9(10) | 0.7(7) |

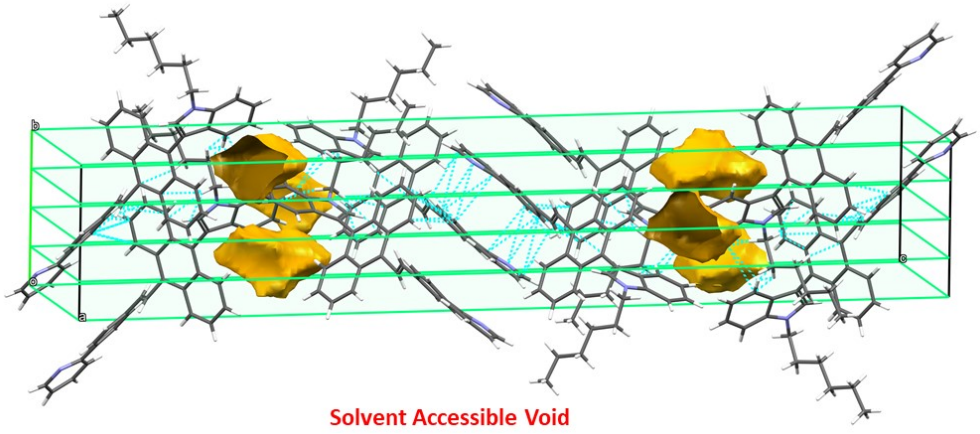


**Fig. S11** Surface accessible void of **IAPY**

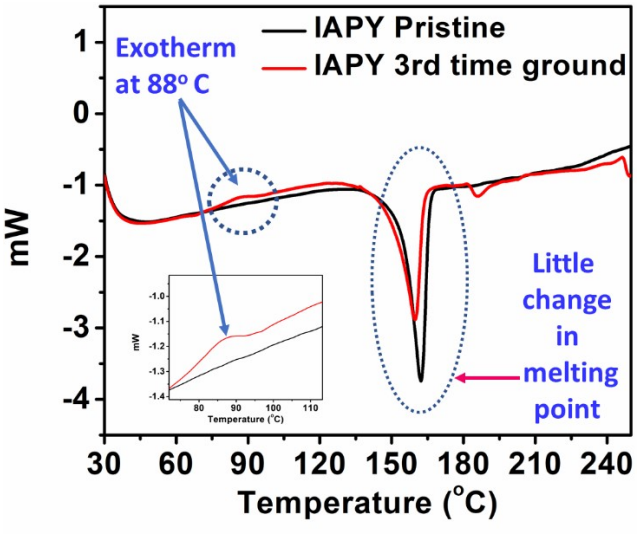


**Fig. S12** DSC for the 3rd time ground form of **IAPY**

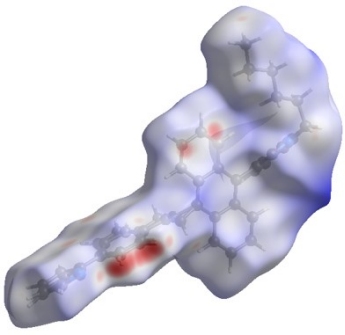

**Fig. S13** Hirshfeld surface of **IAPY**

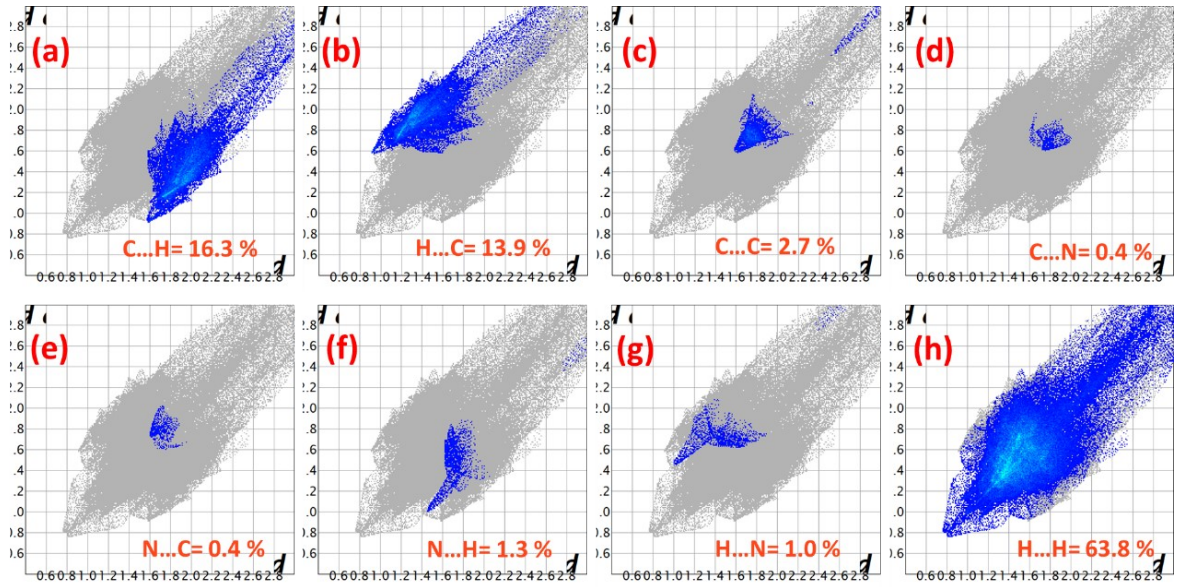


**Fig. S14** Hirshfeld surface and van der Waals and the non-covalent interactions to the packing for **IAPY**

**Table S4** Inter-molecular potentials

Calculated inter-molecular potentials:
mol1 mol2 distance energy (kJ/mol)
0 1 8.5606 -56.7549
2 3 8.5606 -56.7549
4 5 8.5606 -56.7549
0 6 16.464 -56.1803
2 7 16.464 -56.1803
8 3 16.464 -56.1803
0 2 8.66273 -53.916
9 10 8.66273 -53.916
11 7 8.66273 -53.916
12 13 8.66273 -53.916
7 6 8.66273 -53.916
1 3 8.66273 -53.916
4 14 8.66273 -53.916

Hydrogen normalisation: On

Cluster Energy:
Cluster 1
PE = -122.19 kJ/mol 39 interactions
PE = -124.06 kJ/mol 119 interactions
PE = -124.16 kJ/mol 159 interactions
PE = -124.18 kJ/mol 179 interactions
PE = -124.19 kJ/mol 189 interactions
PE = -124.19 kJ/mol 199 interactions
Cluster 2
PE = -310.85 kJ/mol 39 interactions
PE = -319.49 kJ/mol 119 interactions

PE = -320.21 kJ/mol 159 interactions
PE = -320.42 kJ/mol 179 interactions
PE = -320.50 kJ/mol 189 interactions
PE = -320.55 kJ/mol 199 interactions

Total packing energy = -444.7 kJ/mol

Potential = A*exp(-Br) - Cr(-6)

Unified (UNI) pair-potential parameters:
atom1 code1 atom2 code2 A B C
C15 3 C15 3 226145.2 3.47 2418.0
C15 3 N5 23 491494.0 3.86 2791.0
C15 3 H27 1 120792.1 4.10 472.8
N5 23 N5 23 365263.0 3.65 2891.0
N5 23 H27 1 228279.0 4.52 502.1
H27 1 H27 1 24158.0 4.01 109.2

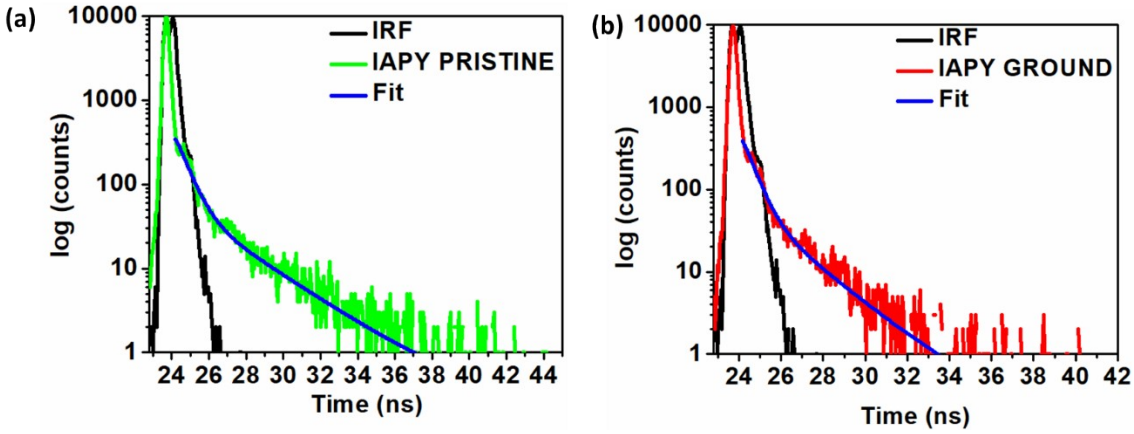


**Fig. S15** Decay profile of **IAPY** for MIEE property

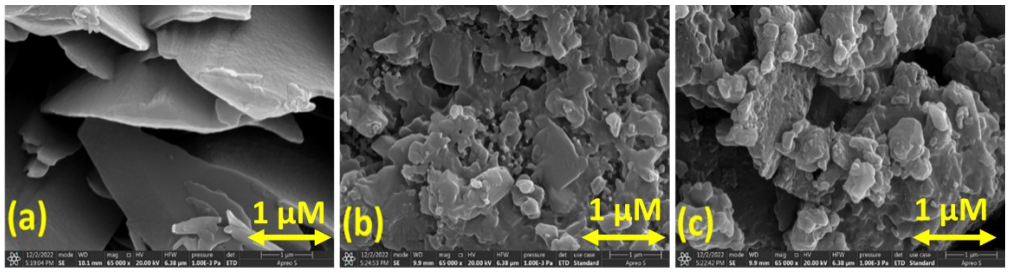


**Fig. S16** SEM images for **IAPY** (a) pristine (b) ground (c) recovered

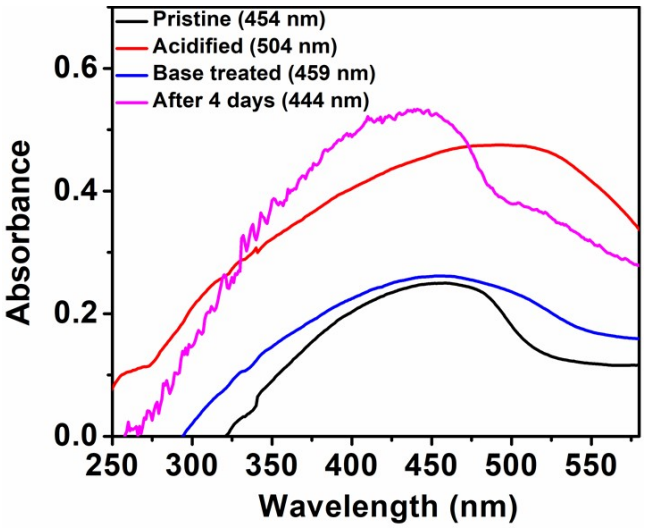


**Fig. S17** Absorbances for **IAPY** SSAC

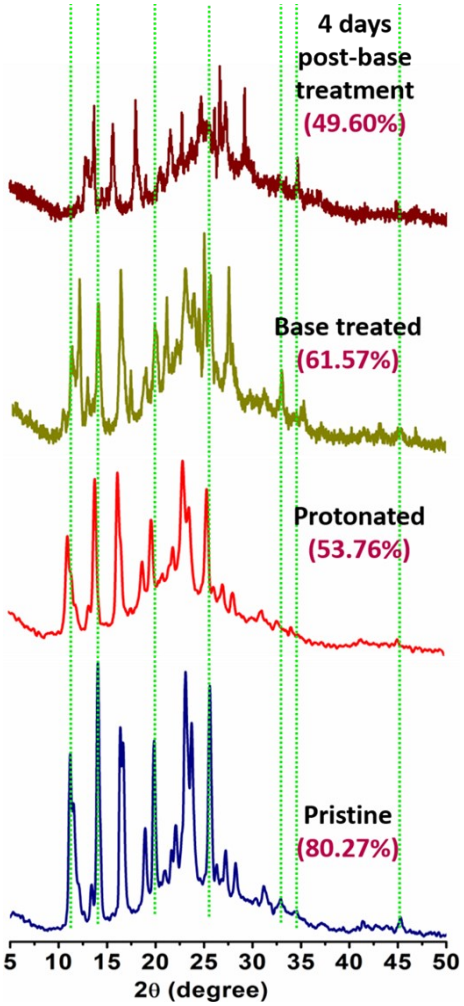


**Fig. S18a** Changes in PXRD pattern for **IAPY** due to acidofluorochromism

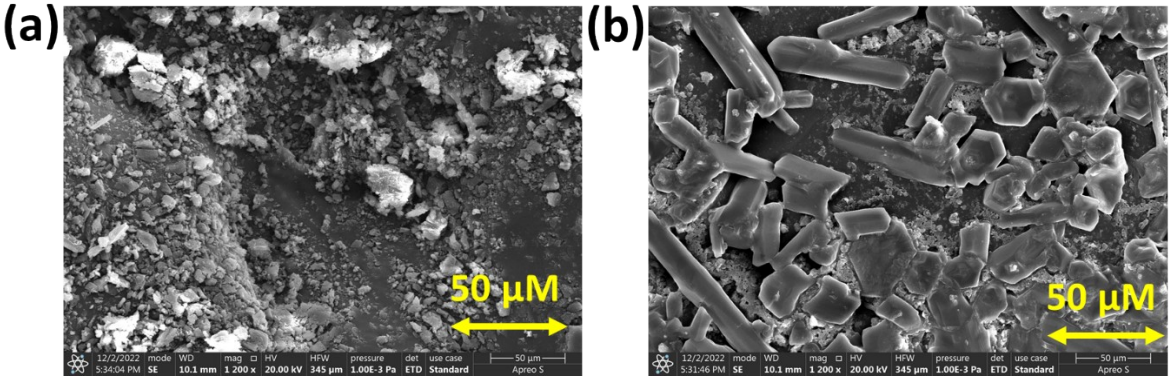


**Fig. S18b** SEM images for **IAPY** (a) acid-fumed (b) base-fumed

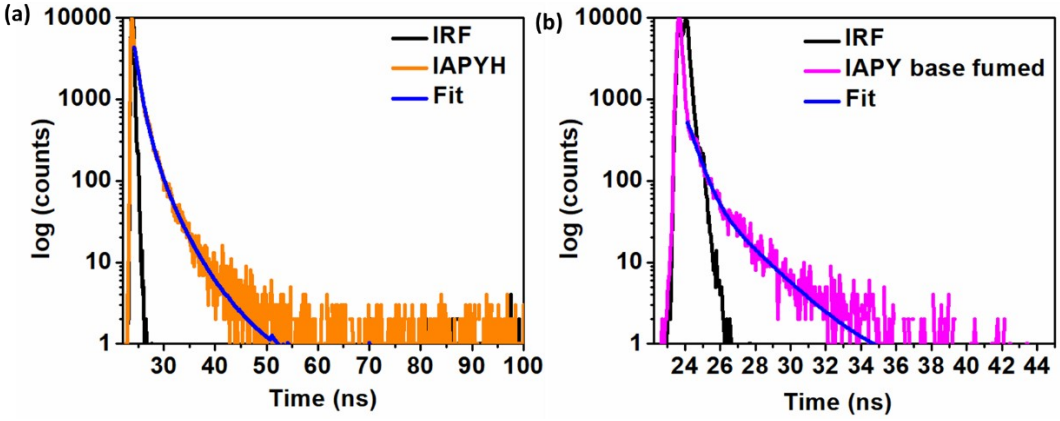


**Fig. S19** Decay profile for **IAPY** (a) acid-fumed (**IAPYH**) (b) base-fumed

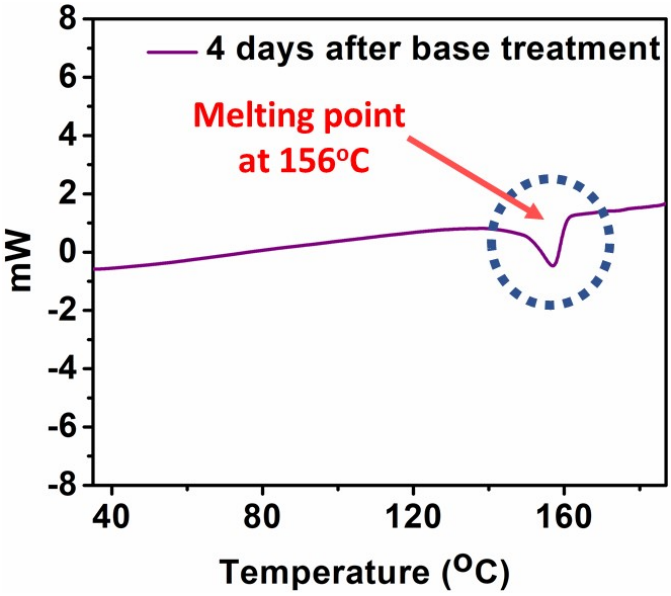


**Fig. S20** DSC for the '4th day post to base treatment' form of **IAPY**

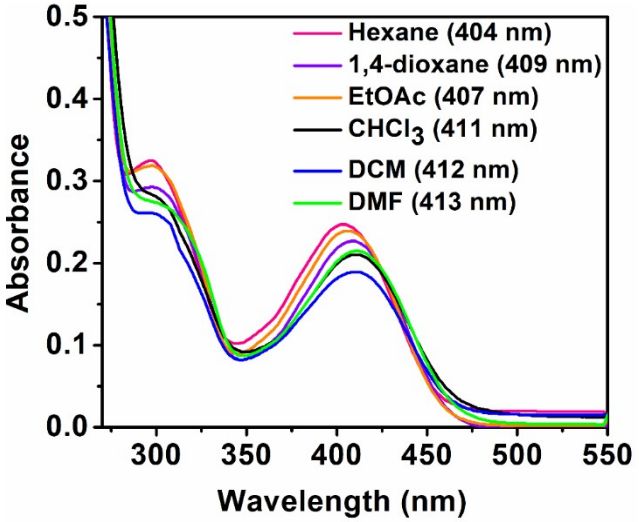


**Fig. S21** Absorbances of **IAPY** in different solvents

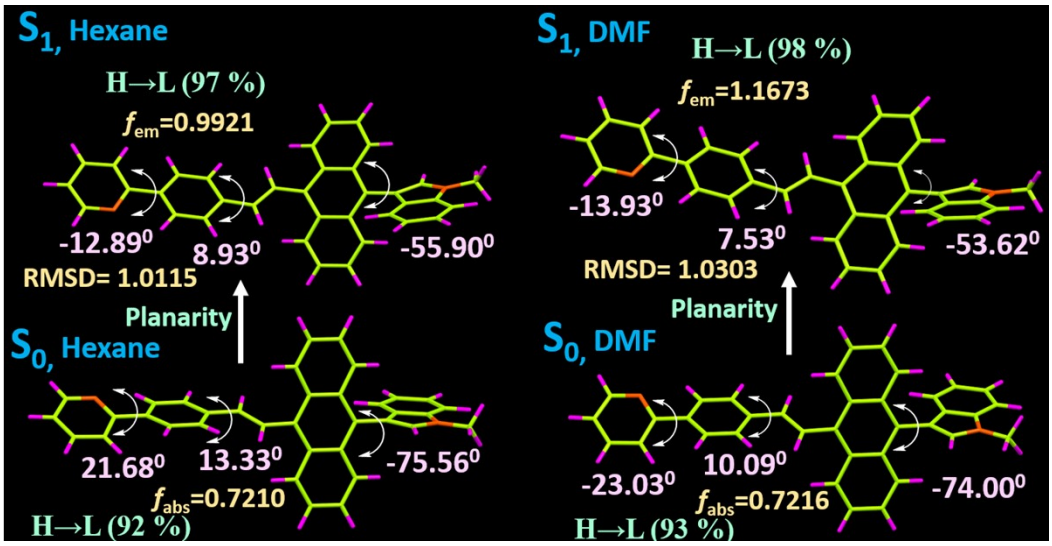


**Fig. S22** TD-DFT optimized structures and calculations for IAPY in Hexane and N,N-DMF using CAM-B3LYP/6-31G* level of theory.

Cyclic voltammetry study

Procedure and calculation: The HOMO/LUMO energy levels were calculated from the oxidation onset/reduction potentials in due course of positive/negative scans. For **IAPY,** $10^{-5}$ M of DCM (dichloromethane) and $10^{-5}$M of *N,N*-DMF (dimethylformamide) solution were used with glassy carbon (GC) electrode as working electrode (WE) along with the Pt-wire and Ag/AgCl were used as a counter electrode (CE) and reference electrode (RE) respectively with a 0.1 M tetrabutylammonium perchlorate (TBAP) in the respective solvents as an electrolyte in a typical three-electrode system at normal condition.

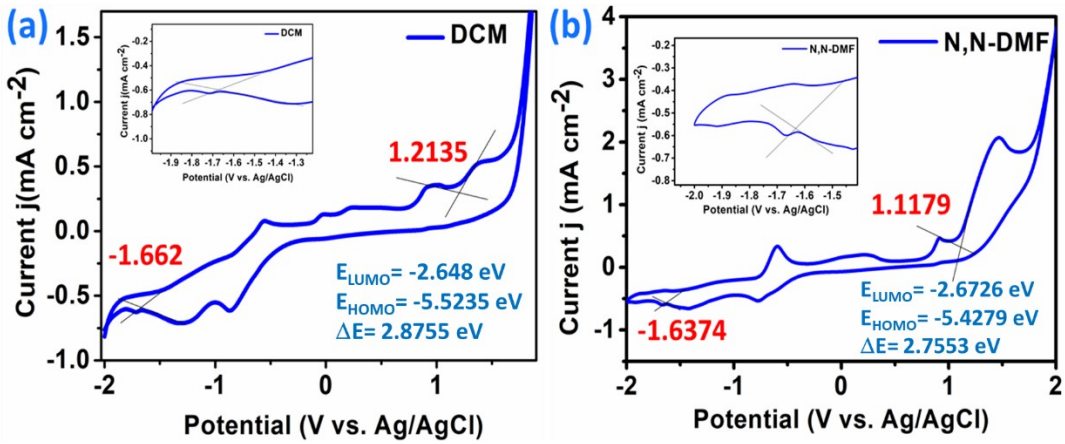


**Fig. S23a** HOMO-LUMO calculation from CV for **IAPY** in (a) DCM, and (b) N,N-DMF

$E_{HOMO}$(DCM) =- ($E^{OX}_{Onset}$- 0.49 + 4.8) eV = - (1.2135- 0.49 + 4.8) eV = -5.5235 eV

$E_{LUMO}$(DCM) = - ($E^{Red}_{Onset}$- 0.49 + 4.8) eV = - (-1.662- 0.49 + 4.8) eV = -2.648 eV

Energy Gap (DCM) = $E_{LUMO}$- $E_{HOMO}$ = (-2.648 + 5.5235) eV = 2.8755 eV

Again,

$E_{HOMO}$(DMF) = - ($E^{OX}_{Onset}$- 0.49 + 4.8) eV = - (1.1179- 0.49 + 4.8) eV = -5.4279 eV

$E_{LUMO}$(DMF) = - ($E^{Red}_{Onset}$- 0.49 + 4.8) eV = - (-1.6374- 0.49 + 4.8) eV = -2.6726 eV

Energy Gap (DMF) = $E_{LUMO}$- $E_{HOMO}$ = (-2.6726 + 5.4279) eV = 2.7553 eV

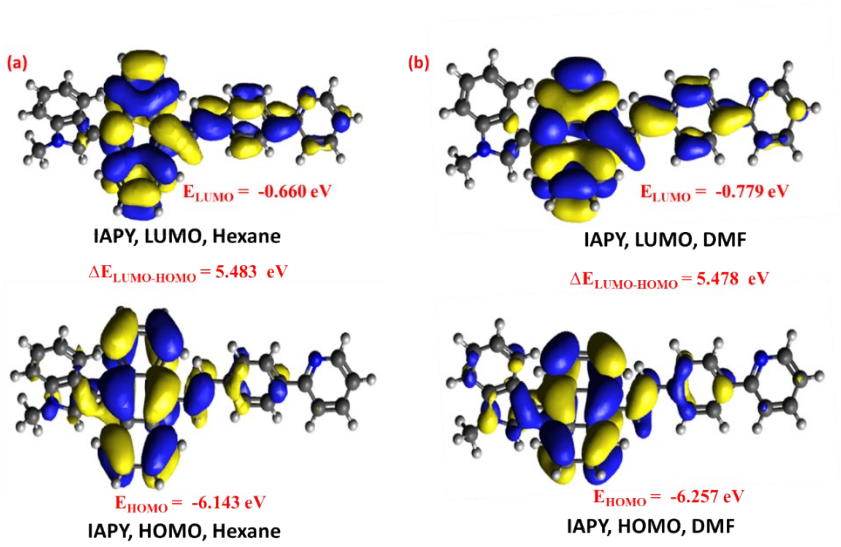


**Fig. S23b** HOMO-LUMO for **IAPY** in Hexane and DMF using CAM-B3LYP/6-31G*

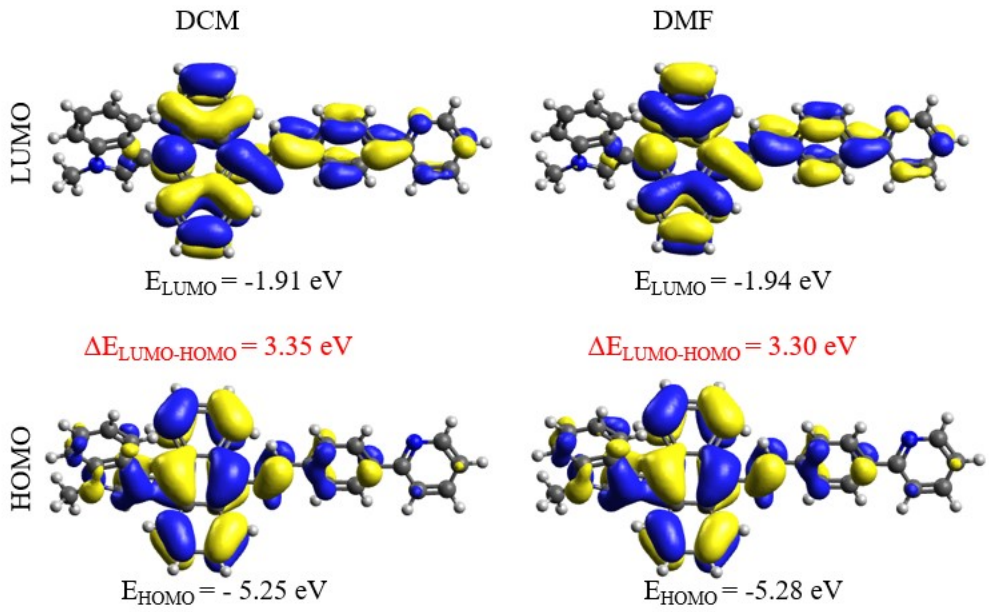


**Fig. S23c** HOMO-LUMO for **IAPY** in Hexane and DMF using PBE0/6-31G* level of theory

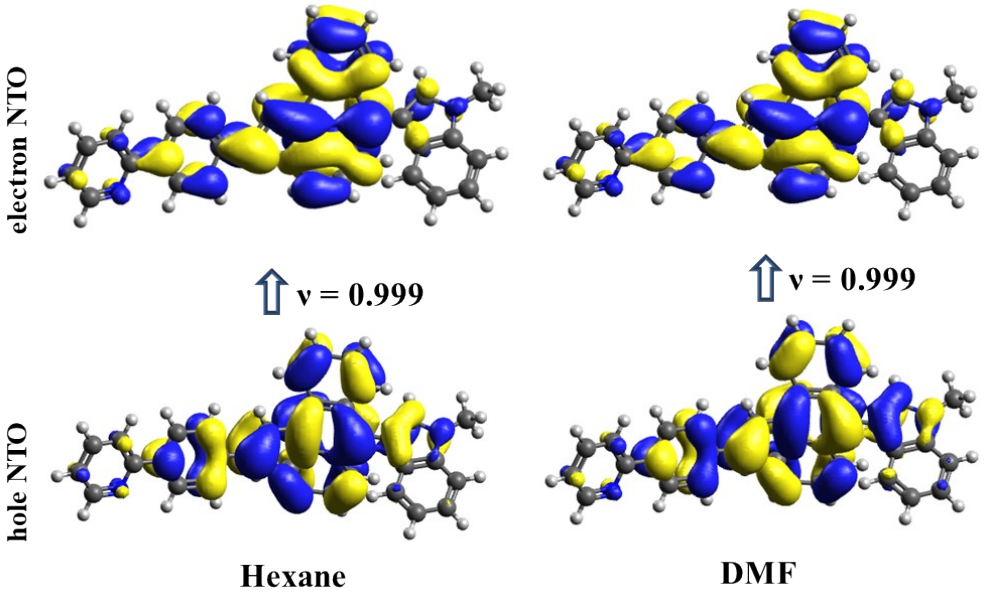


**Fig. S23d** NTOs for **IAPY** in Hexane and DMF using CAM-B3LYP/6-31G*

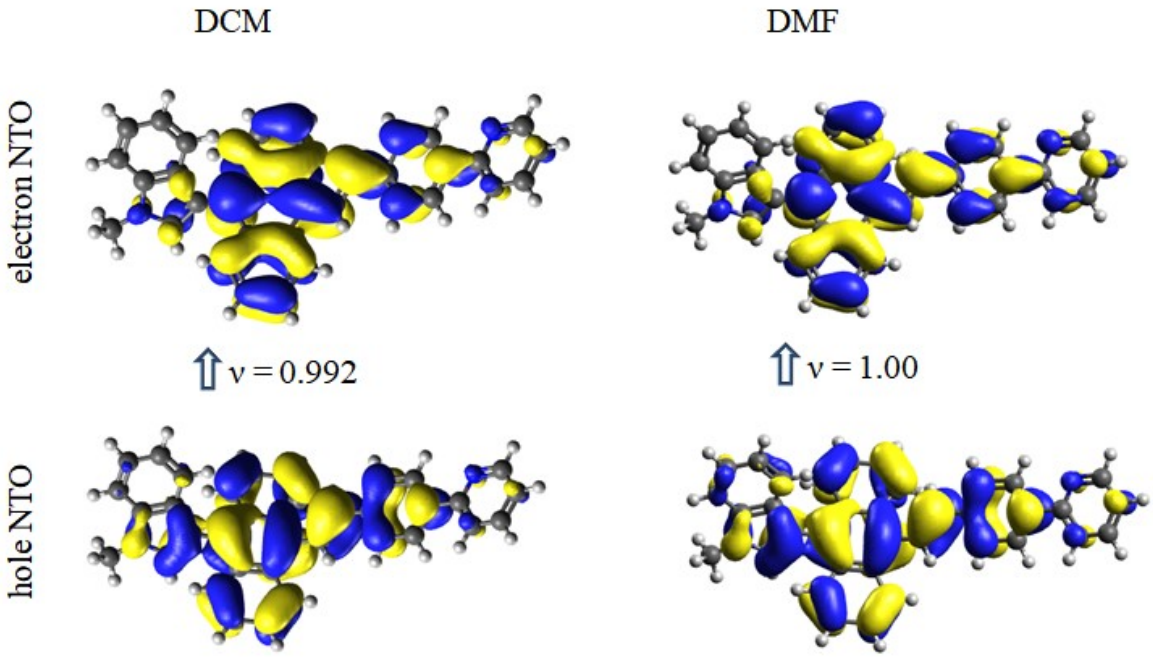


**Fig. S23e** Hole and electron NTOs in the $S_1$ state of **IAPY** in DCM and DMF solvent with PBE0/6-31G* level of theory

**Table S5** Calculation of Electronic Properties in DFT and DCM Solvent

| Properties/ Functionals | **B3LYP** | **CAM-B3LYP** | **M062X** | **BHnadHLYP** | **PBE0** | **WB97X** |
|---|---|---|---|---|---|---|
| HOMO (DMF) | -4.9482 | -6.2572 | -6.1992 | -5.8986 | -5.2752 | -7.18 |
| LUMO (DMF) | -1.8683 | -0.779 | -1.2049 | -0.8648 | -1.9327 | 0.019 |
| **Energy gap (DMF)** | **3.080** | **5.478** | **4.994** | **5.034** | **3.343** | **7.199** |
| HOMO (DCM) | -4.9274 | -6.2353 | -6.2675 | -5.8744 | -5.2505 | -7.1559 |
| LUMO (DCM) | -1.8461 | -0.7561 | -1.1696 | -0.8399 | -1.9057 | 0.0456 |
| **Energy gap (DCM)** | **3.081** | **5.479** | **5.098** | **5.035** | **3.345** | **7.202** |

To bring clarity, we have calculated the $S_0$ state HOMO-LUMO energy gap using the different functions enlisted above.

**Table S6** Optimized Ground State ($S_0$) Geometry in DCM solvent

| CAM-B3LYP/6-31G* | | | PBE0/6-31G* | | |
|---|---|---|---|---|---|
| C | 1.07347291682372 | 3.88433021727958 | 0.42451449178687 | C | 1.09675809495630 | 3.94076758973123 | 0.29174089804622 |
| C | 2.49350070384042 | 3.83698551135463 | 0.47306915401305 | C | 2.51291162068535 | 3.88593439739794 | 0.34858260806975 |
| C | 3.14904229923654 | 2.67540096307094 | 0.19775084156227 | C | 3.16306268548559 | 2.70543882965744 | 0.11611257177854 |
| C | 2.44190210324303 | 1.48111278548665 | -0.15655914231186 | C | 2.45048908230953 | 1.50850662508112 | -0.20244795149290 |
| C | 1.00872589136294 | 1.52924306062491 | -0.20981696836379 | C | 1.01294700008879 | 1.56331464105161 | -0.26148099643988 |
| C | 0.36126925420874 | 2.76829466529378 | 0.10308607963833 | C | 0.37522784686478 | 2.81322945416165 | 0.00807829957909 |
| C | 3.11892637761039 | 0.27478190422099 | -0.42326876480818 | C | 3.12348640985442 | 0.28589168281792 | -0.41937250371791 |
| C | 2.37883399020110 | -0.87660069649140 | -0.75347808449077 | C | 2.37528956815091 | -0.87417791292036 | -0.71582295623856 |
| C | 0.94301439881026 | -0.82903571249970 | -0.82218321425391 | C | 0.93588869441062 | -0.82140794403248 | -0.79094590699058 |
| C | 0.26533236431603 | 0.37371880750948 | -0.53136035353027 | C | 0.25953990333077 | 0.39643448982317 | -0.53718972053350 |
| C | 3.03575393596665 | -2.11432730185689 | -1.05568372677117 | C | 3.02738481107403 | -2.11727033904051 | -0.98658849558119 |
| C | 2.33539278005498 | -3.22490584291252 | -1.41376679096456 | C | 2.32149563800939 | -3.23829108141187 | -1.32324222885219 |
| C | 0.91784894908563 | -3.17084747905852 | -1.51434851167674 | C | 0.90838394969629 | -3.17904057943907 | -1.43489334929189 |
| C | 0.25222297136738 | -2.01695881072710 | -1.23268018736188 | C | 0.24429741366029 | -2.01045383499373 | -1.18194836491111 |
| C | -1.21000952835334 | 0.47171008454059 | -0.58266508400646 | C | -1.20713163101175 | 0.49733405193351 | -0.57844379178990 |
| C | -2.05668883067337 | -0.30400573456424 | 0.10621356585420 | C | -2.06074815724340 | -0.30732569385619 | 0.08338843151809 |
| C | -3.52464122775007 | -0.22876990208648 | 0.08812769452386 | C | -3.52090584351502 | -0.22901920490326 | 0.07189911326763 |
| C | 4.59792956498018 | 0.20626702182805 | -0.34265848739182 | C | 4.59605905769347 | 0.21095042790740 | -0.32717872530006 |
| C | 5.38136707453010 | -0.39941976507822 | 0.70515895519634 | C | 5.37209591469378 | -0.43890017902373 | 0.69692361364202 |
| C | 6.74115793990797 | -0.22801349369138 | 0.35568019354544 | C | 6.73847794313934 | -0.24408693219780 | 0.36698739391262 |
| N | 6.78893182080616 | 0.44667190805800 | -0.84257172160215 | N | 6.79170533582546 | 0.48335995907054 | -0.79739590120849 |
| C | 5.49988795674845 | 0.69978006353582 | -1.24758361963616 | C | 5.50937868869622 | 0.75201905993750 | -1.20248474319621 |
| C | 5.06164170436113 | -1.06375005647281 | 1.89810478086589 | C | 5.04744990275500 | -1.15502871339813 | 1.85936273964629 |
| C | 6.08758004091065 | -1.53427578359152 | 2.69837329751746 | C | 6.07342825420314 | -1.65313682779107 | 2.64825341925485 |
| C | 7.43590166049439 | -1.35388470737124 | 2.33262895652473 | C | 7.42381160015771 | -1.44920366407882 | 2.30234570610782 |
| C | 7.78147449171555 | -0.70123086381787 | 1.16165958299959 | C | 7.77587616850363 | -0.74361766943563 | 1.16023971362773 |
| C | 7.99382077677895 | 0.80578116349947 | -1.56055746906685 | C | 7.99929440908851 | 0.87878119368254 | -1.48384004820009 |
| C | -4.24571604198201 | 0.56849285979158 | -0.81068839449402 | C | -4.24930788123358 | 0.61082774784401 | -0.78777390546940 |
| C | -5.63054093329171 | 0.60924922710488 | -0.77691471357566 | C | -5.63454034517169 | 0.64950920651695 | -0.74608737358999 |
| C | -6.35447179714612 | -0.14784319854742 | 0.15246685717531 | C | -6.35781714367768 | -0.15184690692216 | 0.15155407319908 |
| C | -5.63879217698574 | -0.95651392452219 | 1.03953039938692 | C | -5.63578787686443 | -1.00275941632865 | 0.99844995976041 |
| C | -4.25307205272181 | -0.99401992468059 | 1.00712762174553 | C | -4.24962978409465 | -1.03848995906042 | 0.95880153535980 |
| H | 0.55757777715496 | 4.81087715830113 | 0.65676500171717 | H | 0.58366395313587 | 4.87795479868118 | 0.49038223669266 |
| H | 3.05237932146487 | 4.72816777770488 | 0.74149178042555 | H | 3.07886622221516 | 4.78116691991673 | 0.59203617372346 |
| H | 4.23024860396985 | 2.63482246186236 | 0.24791024987191 | H | 4.24505016294826 | 2.65738329478869 | 0.17885216921260 |
| H | -0.72154710021132 | 2.81018573083889 | 0.09737207270248 | H | -0.70865005523285 | 2.86484110902271 | 0.00394959033906 |
| H | 4.11702774519867 | -2.14758943568299 | -1.00052547666944 | H | 4.11034631564260 | -2.15163238688717 | -0.93110228086562 |
| H | 2.85675363994718 | -4.14974926617911 | -1.64059576884985 | H | 2.84216756650519 | -4.16977142610403 | -1.52885923772714 |
| H | 0.36709636237017 | -4.05182614877441 | -1.82937348768184 | H | 0.35315861597625 | -4.06226272675012 | -1.73945754486917 |
| H | -0.82434116780475 | -1.98135239052495 | -1.33402156883678 | H | -0.83222811064481 | -1.97121758176665 | -1.30071191003321 |
| H | -1.61043306743673 | 1.26791180304675 | -1.20712953660168 | H | -1.61096327510409 | 1.32242919535697 | -1.16448604802990 |
| H | -1.64643317594969 | -1.06355880770309 | 0.76934192808829 | H | -1.64887112717733 | -1.08926931735189 | 0.72121062637664 |
| H | 5.32050061190783 | 1.22347262113492 | -2.17722306532673 | H | 5.33725706543588 | 1.31541831140455 | -2.11105921112200 |
| H | 4.02368090191730 | -1.20578449215382 | 2.18493998298803 | H | 4.00748886737632 | -1.31659146796556 | 2.13219207366437 |
| H | 5.85373480682168 | -2.05122754827525 | 3.62411633186790 | H | 5.83497019265312 | -2.21046669544770 | 3.55040549600823 |
| H | 8.21878959213242 | -1.73434987880844 | 2.98156361640066 | H | 8.20498887338734 | -1.85174892748332 | 2.94171975360326 |
| H | 8.82080530786655 | -0.56248636689111 | 0.88128421424003 | H | 8.81780299367327 | -0.58564973737287 | 0.89528720982183 |
| H | 8.62572440923082 | 1.46128901322413 | -0.95419108735056 | H | 8.62254601130210 | 1.50695421462112 | -0.83872257212265 |
| H | 7.71520990905045 | 1.33279491947581 | -2.47359959244135 | H | 7.72835691957044 | 1.44800762534838 | -2.37459898074541 |
| H | -6.18349768812007 | -1.55637140368816 | 1.75906703838410 | H | -6.17861513463664 | -1.63629549488360 | 1.69250808130007 |

| | | | | | | | |
|---|---|---|---|---|---|---|---|
| H | -3.71861243040447 | -1.62576632654438 | 1.71144296259104 | H | -3.71186094106091 | -1.70266823687944 | 1.63205840557901 |
| H | -6.15124953778968 | 1.22231542137825 | -1.50493739969233 | H | -6.15760427929118 | 1.29511841661688 | -1.44576077808487 |
| H | -3.72294791350051 | 1.15470603810043 | -1.55936238190652 | H | -3.73039028006898 | 1.23164838499788 | -1.51285950298157 |
| C | -7.83958339738065 | -0.11444296345949 | 0.20465296938715 | C | -7.83748454781612 | -0.12394152912688 | 0.21272322823735 |
| C | -8.57072137035129 | 0.95847607804949 | -0.31588254656841 | C | -8.57824148323229 | 0.95959226715721 | -0.28041618418451 |
| C | -9.77628884290251 | -1.16502940266227 | 0.86327160256431 | C | -9.76526864112198 | -1.19749193071997 | 0.86180203004511 |
| C | -9.95610854031338 | 0.93621401491102 | -0.23974648994440 | C | -9.96470484256108 | 0.92852115361060 | -0.19614865620727 |
| H | -8.06431827803136 | 1.80826768144423 | -0.75765458287328 | H | -8.07964561806118 | 1.82396631069652 | -0.70619367732917 |
| C | -10.58117872948028 | -0.14945380152419 | 0.36098894529248 | C | -10.58153003238311 | -0.17492394560018 | 0.38527746193209 |
| H | -10.22402461517712 | -2.03075469895104 | 1.34667337464271 | H | -10.20597670834142 | -2.07648011003563 | 1.33045140941495 |
| H | -10.53793750212881 | 1.76192332064174 | -0.63741505080904 | H | -10.55357473798964 | 1.76088219223351 | -0.57201779009646 |
| H | -11.66051244945738 | -0.20979943904656 | 0.44575084537476 | H | -11.66115058569300 | -0.24308233591921 | 0.47493337312015 |
| N | -8.44620113032407 | -1.15814521349933 | 0.79092376490745 | N | -8.43564643767042 | -1.18441898265456 | 0.78228204989546 |
| H | 8.56675056927409 | -0.08690250097470 | -1.82880688392331 | H | 8.57821374774403 | 0.00003714071522 | -1.78746101853338 |

**Table S7** Optimized Ground State ($S_0$) Geometry in DMF solvent

| CAM-B3LYP/6-31G* | | | | PBE0/6-31G* | | | |
|---|---|---|---|---|---|---|---|
| C | 1.07093888627897 | 3.88796972042159 | 0.41052875475638 | C | 1.09648913438479 | 3.94344107987493 | 0.27631151842883 |
| C | 2.49090605431695 | 3.84106280373719 | 0.46170443928103 | C | 2.51284677274510 | 3.88881574791157 | 0.33438488409220 |
| C | 3.14725037065322 | 2.67939533127090 | 0.18840429016711 | C | 3.16310978860084 | 2.70767660866717 | 0.10536593736191 |
| C | 2.44116580656204 | 1.48450555249168 | -0.16630480612701 | C | 2.45064254119061 | 1.50962917513585 | -0.21054750577161 |
| C | 1.00790120728462 | 1.53212008839476 | -0.22175573258155 | C | 1.01300537779912 | 1.56417817130300 | -0.27056647518030 |
| C | 0.35959704759785 | 2.77137840613271 | 0.08889309061136 | C | 0.37509040925243 | 2.81516714477546 | -0.00492271266823 |
| C | 3.11921194504257 | 0.27812062258142 | -0.43095203531994 | C | 3.12412305988216 | 0.28647915523500 | -0.42408423893409 |
| C | 2.37981887575905 | -0.87314674846087 | -0.76377720305225 | C | 2.37606193703601 | -0.87393257686176 | -0.72013594296066 |
| C | 0.94398333805528 | -0.82619815327737 | -0.83402293316544 | C | 0.93660605191259 | -0.82158502580669 | -0.79558131489507 |
| C | 0.26517438759075 | 0.37594187865665 | -0.54285330049566 | C | 0.25963737990913 | 0.39634730247476 | -0.54325907817879 |
| C | 3.03760845032971 | -2.11007361446228 | -1.06772120342736 | C | 3.02858212261544 | -2.11727692404315 | -0.99020595980416 |
| C | 2.33827960335671 | -3.22043955669151 | -1.42873389792597 | C | 2.32325499061396 | -3.23878274049541 | -1.32663764473208 |
| C | 0.92076303128912 | -3.16706672552267 | -1.53018499039261 | C | 0.90988770082107 | -3.18001354117881 | -1.43835205869870 |
| C | 0.25427402457240 | -2.01401023645581 | -1.24683757094936 | C | 0.24547605708463 | -2.01145252840355 | -1.18589943127730 |
| C | -1.21041749612565 | 0.47199170613327 | -0.59199784291114 | C | -1.20714888677004 | 0.49655573859615 | -0.58218949419560 |
| C | -2.05359036237298 | -0.30664782121203 | 0.09793985368722 | C | -2.05960292493404 | -0.30934221154744 | 0.07982565058285 |
| C | -3.52169220086039 | -0.23352199168547 | 0.08378927930814 | C | -3.51985305455798 | -0.23031348256265 | 0.07105363574255 |
| C | 4.59779005691942 | 0.20863140153145 | -0.34416470462557 | C | 4.59652464338852 | 0.21106923631759 | -0.32794048184164 |
| C | 5.37444947660482 | -0.40283931573825 | 0.70536438622299 | C | 5.36892050608699 | -0.44018832170590 | 0.69806738484330 |
| C | 6.73657355748032 | -0.23054014529157 | 0.36490666764638 | C | 6.73651951067830 | -0.24458050623185 | 0.37279951702525 |
| N | 6.79186978481590 | 0.44976586523296 | -0.82974603337441 | N | 6.79371036353601 | 0.48420052084089 | -0.79046039818996 |
| C | 5.50576737864936 | 0.70620721899826 | -1.24109626644151 | C | 5.51314968597104 | 0.75331211123933 | -1.19948252838341 |
| C | 5.04743642956197 | -1.07228880971488 | 1.89360287109180 | C | 5.04065461555274 | -1.15782733021365 | 1.85886786256495 |
| C | 6.06842134487602 | -1.54661390511505 | 2.69813822300740 | C | 6.06425017737837 | -1.65660622919143 | 2.65077841116130 |
| C | 7.41910045556080 | -1.36504920244941 | 2.34140386379104 | C | 7.41592666766383 | -1.45180107330196 | 2.30941600985412 |
| C | 7.77188199204358 | -0.70751020847727 | 1.17521210768046 | C | 7.77149397420941 | -0.74476252855227 | 1.16909071284635 |
| C | 8.00162875401639 | 0.81295149667056 | -1.53859640985137 | C | 8.00396147805325 | 0.88148394871315 | -1.47247416094574 |
| C | -4.24630555336725 | 0.54779934270085 | -0.82618000646267 | C | -4.24945114285674 | 0.61320797580336 | -0.78425294634858 |
| C | -5.63106719219553 | 0.58900905637185 | -0.78762199913041 | C | -5.63474954741672 | 0.65197253763740 | -0.74033896502680 |
| C | -6.35082281300431 | -0.15221573982564 | 0.15771725814985 | C | -6.35684601855955 | -0.15308209375534 | 0.15514083655789 |
| C | -5.63170702537671 | -0.94581404510049 | 1.05555531611826 | C | -5.63343681143554 | -1.00689809430874 | 0.99825069237270 |
| C | -4.24600176528502 | -0.98378201142249 | 1.01831604186811 | C | -4.24720116063883 | -1.04283273691432 | 0.95645130495451 |
| H | 0.55439424136316 | 4.81474491905235 | 0.64041776067154 | H | 0.58318770963310 | 4.88129907730332 | 0.47127024470717 |
| H | 3.04902980816742 | 4.73276585835772 | 0.72999802851460 | H | 3.07868492792648 | 4.78490305942610 | 0.57501234586084 |
| H | 4.22842730737112 | 2.63964561863247 | 0.24000350813036 | H | 4.24519303780460 | 2.66034178631688 | 0.16761425275906 |
| H | -0.72319079584309 | 2.81379039962345 | 0.08056263362647 | H | -0.70875127866802 | 2.86796024601234 | -0.01139536441943 |
| H | 4.11889397173037 | -2.14274575148090 | -1.01237176749085 | H | 4.11162530679082 | -2.15117912866819 | -0.93514121194934 |
| H | 2.86037486847178 | -4.14441146305238 | -1.65748159162264 | H | 2.84429343228563 | -4.17012508390662 | -1.53209529882522 |
| H | 0.37075634953338 | -4.04771400571202 | -1.84744720784024 | H | 0.35485714161805 | -4.06342542642076 | -1.74277204871142 |
| H | -0.82225095990221 | -1.97929490588773 | -1.34889283142183 | H | -0.83110502877960 | -1.97331825283001 | -1.30463545801095 |
| H | -1.61427402780504 | 1.26851734856567 | -1.21381578031207 | H | -1.61250903284307 | 1.32251968727916 | -1.16591014533888 |
| H | -1.64009155941790 | -1.06574214375891 | 0.75962447231035 | H | -1.64716849253345 | -1.09285609655651 | 0.71542979500775 |
| H | 5.33336779689950 | 1.23468239117876 | -2.16939964025732 | H | 5.34483341444845 | 1.31836752412211 | -2.10782930086837 |
| H | 4.00778448175250 | -1.21559082001159 | 2.17390448502920 | H | 3.99983958088539 | -1.32014490854783 | 2.12844684586284 |
| H | 5.82875567039796 | -2.06745875972164 | 3.62026832989937 | H | 5.82297136636084 | -2.21503450081412 | 3.55160018964441 |
| H | 8.19798559717928 | -1.74843453764894 | 2.99346761034415 | H | 8.19524689883349 | -1.85474434794040 | 2.95088061666195 |
| H | 8.81283481932548 | -0.56767446997092 | 0.90149249505878 | H | 8.81419345331725 | -0.58603343253775 | 0.90760846336535 |
| H | 8.62750013313760 | 1.46839869613702 | -0.92611935820468 | H | 8.62376787542995 | 1.50970609408456 | -0.82432907682836 |
| H | 7.72815470372106 | 1.34093874507030 | -2.45254871998500 | H | 7.73535491552836 | 1.45082655827173 | -2.36378673094657 |
| H | -6.17232733825882 | -1.53366866406451 | 1.78806616866331 | H | -6.17441184230826 | -1.64253671864074 | 1.69192849244032 |
| H | -3.70842030005823 | -1.60335812697738 | 1.73103302622603 | H | -3.70845846758035 | -1.70942998920325 | 1.62661297624875 |
| H | -6.15615045835462 | 1.18870353963817 | -1.52369197816504 | H | -6.15879252363157 | 1.30085639558573 | -1.43625131341116 |
| H | -3.72609670821571 | 1.11995921528257 | -1.58745444783513 | H | -3.73162884396191 | 1.23737371257380 | -1.50727761915784 |
| C | -7.83582237763717 | -0.11719109892976 | 0.21453835895376 | C | -7.83676213944198 | -0.12521723352215 | 0.21732363504087 |
| C | -8.56578248762276 | 0.95686254531976 | -0.30497938650589 | C | -8.57664965873206 | 0.96384301435935 | -0.26455566718110 |
| C | -9.77285838128956 | -1.16280579207707 | 0.88006079762519 | C | -9.76573484503527 | -1.20370240251687 | 0.85662827609968 |
| C | -9.95107443665533 | 0.93783842629357 | -0.22494848972075 | C | -9.96324464042145 | 0.93334132086820 | -0.17976459483402 |
| H | -8.05748468794234 | 1.80455291921699 | -0.74872177500489 | H | -8.07744493045501 | 1.83178659787606 | -0.68237037876820 |
| C | -10.57665420784200 | -0.14594688549296 | 0.37881863676887 | C | -10.58095347577475 | -0.17530101611126 | 0.39096624181677 |
| H | -10.22168320143112 | -2.02677644455510 | 1.36561270900921 | H | -10.20755613023971 | -2.08686928786893 | 1.31630328712576 |
| H | -10.53236663106690 | 1.76431846346558 | -0.62173571730353 | H | -10.55142001071731 | 1.77000022884462 | -0.54703115964093 |
| H | -11.65585862121385 | -0.20406778768006 | 0.46659281614115 | H | -11.66060152813220 | -0.24328073561445 | 0.48042025005616 |
| N | -8.44257459249720 | -1.15933665613995 | 0.80388381020940 | N | -8.43568586518813 | -1.19121581528567 | 0.77639565498920 |
| H | 8.57785617337329 | -0.07834200609166 | -1.80386746266520 | H | 8.58453627438472 | 0.00328156461087 | -1.77397021915104 |

**Table S8** DSE properties of **IAPY**

| Compound | Solvent | $ET_{30}$ | $\lambda_{abs.max}$ (nm) | $\lambda_{em.max}$ (nm) | Stokes shift ($cm^{-1}$) | $\Phi_f$ (%) |
|---|---|---|---|---|---|---|
| **IAPY** with $\lambda_{em.max}$ (Solid) = 517 nm | Hexane | 31.0 | 404 | 515 | 90090.09 | 20.22 |
| | 1,4-dioxane | 36.0 | 409 | 518 | 91743.119 | 17.73 |
| | EtOAc | 38.1 | 407 | 522 | 86956.521 | 14.54 |
| | $CHCl_3$ | 39.1 | 411 | 521 | 90909.09 | 13.33 |
| | DCM | 40.7 | 412 | 514 | 98039.216 | 12.79 |
| | N,N-DMF | 43.2 | 413 | 526 | 88495.575 | 9.79 |

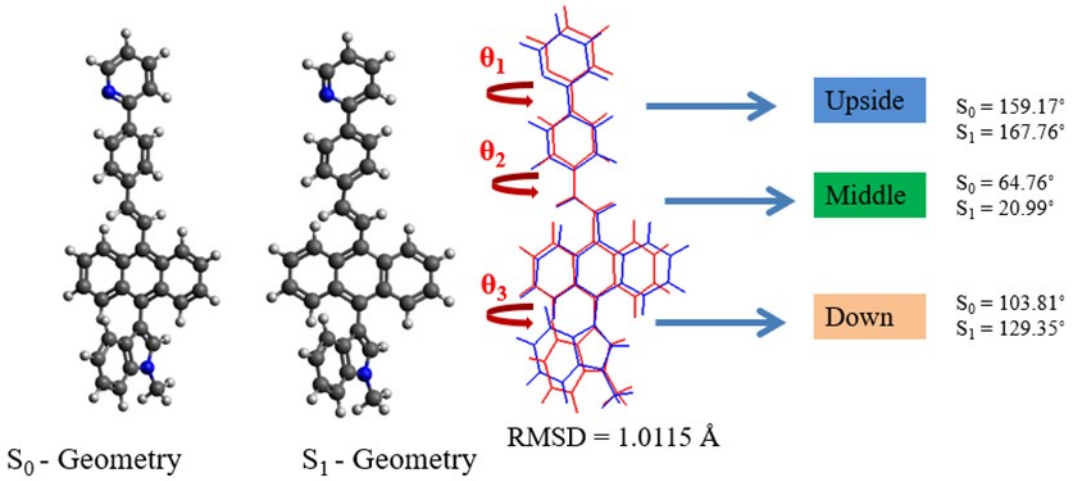


**Fig. S24** Geometry comparison between Ground state ($S_0$) geometry and $S_1$-state optimized geometry IAPY in DMF using CAM-B3LYP/6-31G* level of theory.

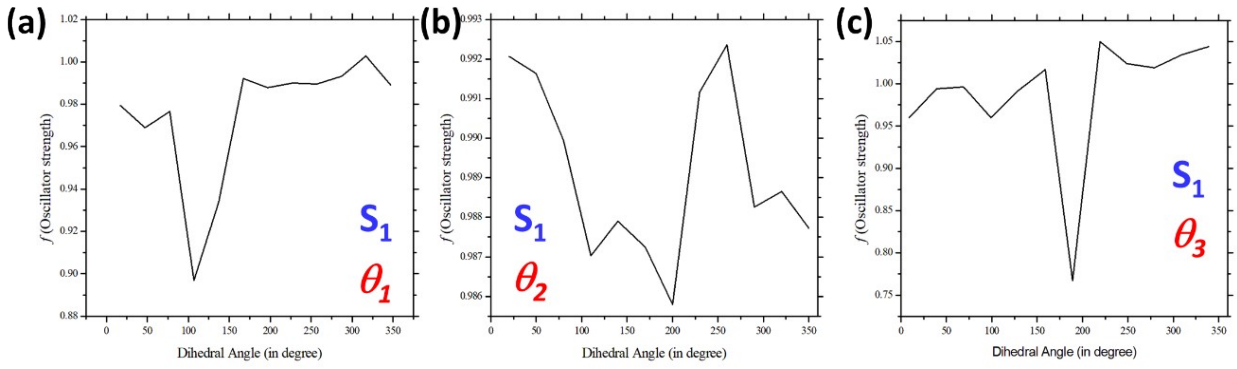


**Fig. S25** Dihedral scanning for emission oscillator strength at different twisted sites of **IAPY**

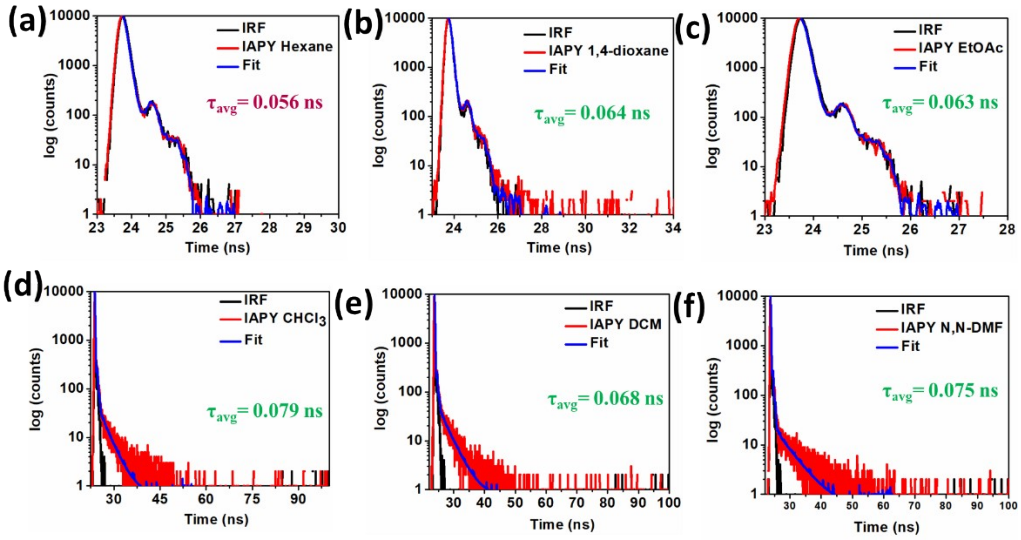


**Fig. S26** Decay profiles of **IAPY** in different solvents

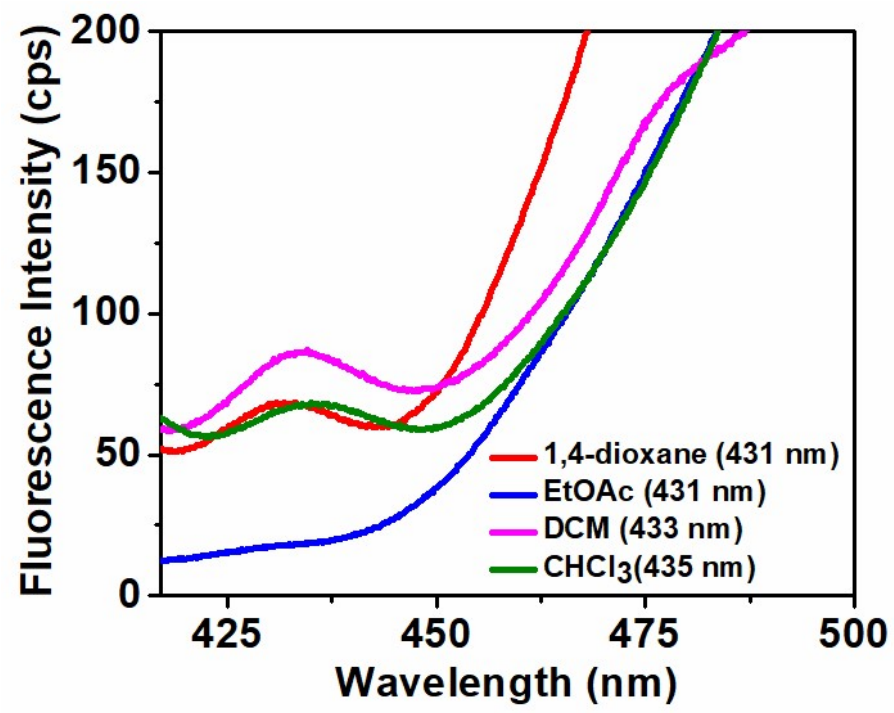


**Fig. S27** LE state emissions of **IAPY** in different solvents

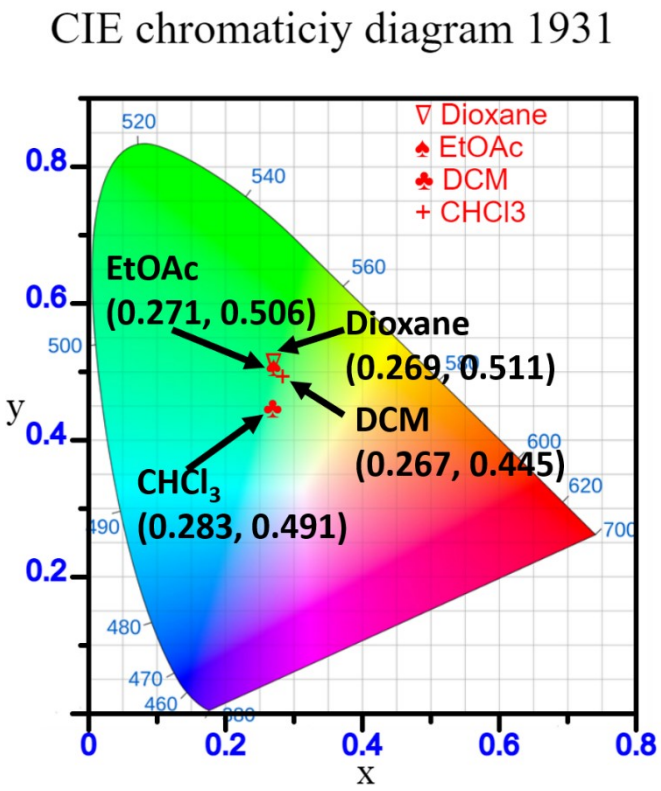


**Fig. S28** CIE-coordinates of whitish emission of **IAPY**

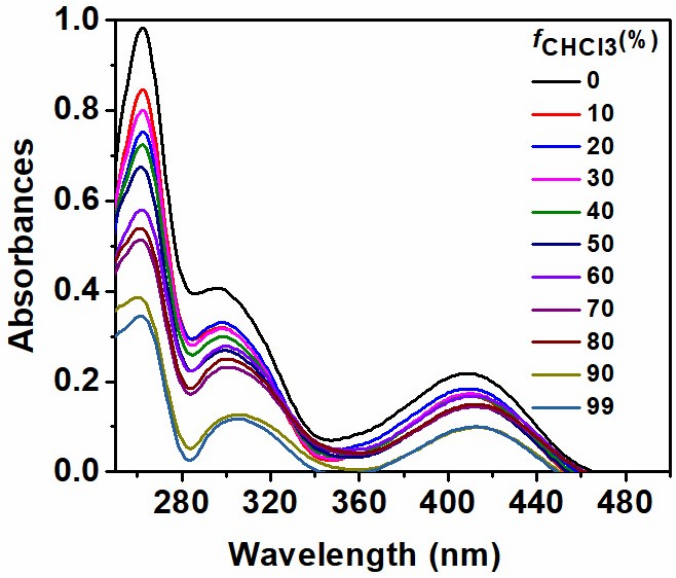


**Fig. S29a** Absorbances for whitish emission for **IAPY** in the binary mixture of 1,4-dioxane and $CHCl_3$.

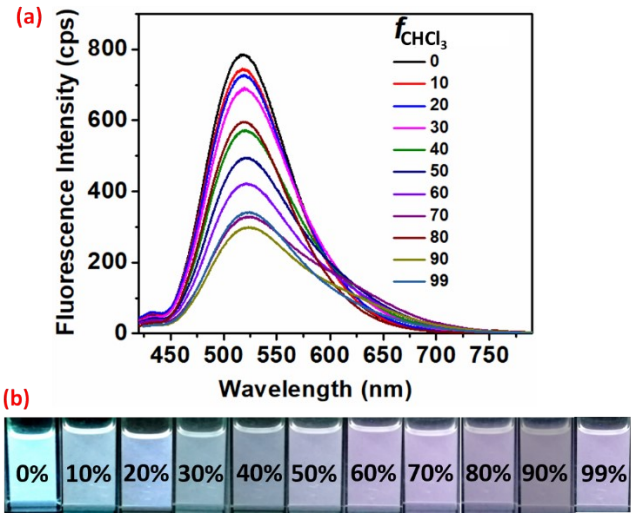


**Fig. S29b** Whitish emission for **IAPY** in the binary mixture of 1,4-dioxane and $CHCl_3$. (The percentage of $CHCl_3$ has been increased gradually, and the excitation wavelength was in the range of 409-416 nm). The CIE coordinates for 0% to 99% are as: **0% (0.27, 0.52), 10% (0.27, 0.52), 20% (0.28, 0.58), 30% (0.29, 0.52), 40% (0.30, 0.52), 50% (0.32, 0.51), 60% (0.32, 0.50), 70% (0.34, 0.50), 80% (0.39, 0.46), 90% (0.34, 0.51), 99% (0.31, 0.52).**

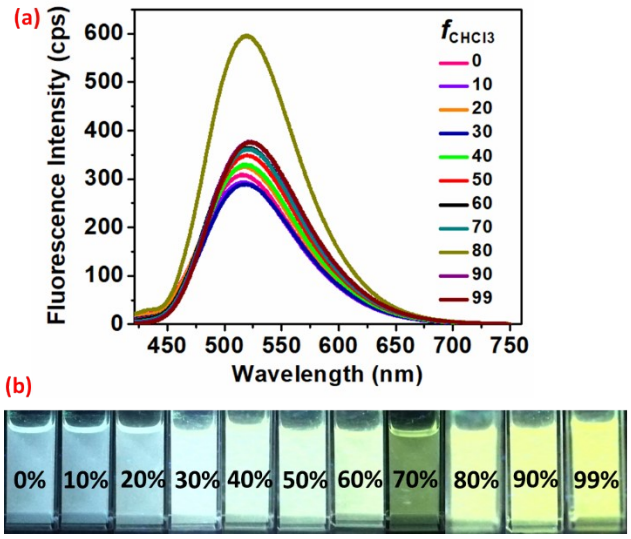


**Fig. S30** Whitish emission for **IAPY** in the binary mixture of EtOAc and $CHCl_3$. (The percentage of $CHCl_3$ has been increased gradually, and the excitation wavelength was in the range of 411-418 nm).

**Table S9** Results of times-resolved studies, altogether

| Compound/Solvent | $\chi^2$ | $\lambda_{em\ max}$ (nm) | $\tau_1$ | $\tau_2$ | $\tau_3$ | $\tau_4$ | α1 | α2 | α3 | α4 | $\tau_{avg.}$ (ns) | $\Phi_f$ (%) | $k_r(s^{-1})$ x $10^{-6}$ | $k_{nr}(s^{-1})$ x $10^{-6}$ |
|---|---|---|---|---|---|---|---|---|---|---|---|---|---|---|
| IAPY Pristine | 1.012 | 517 | 0.6068 | 2.9607 | - | - | 0.9032 | 0.0967 | - | - | 0.8344 | 26.64 | 319.271 | 879.194 |
| IAPY Ground | 1.067 | 534 | 0.4983 | 2.1100 | | - | 0.9079 | 0.0920 | | - | 0.6467 | 53.32 | 824.493 | 721.818 |
| IAPY H | 1.000 | 530 | 0.6004 | 1.4100 | 3.449 | - | 0.6269 | 0.3189 | 0.0531 | - | 1.0237 | 1.16 | 11.331 | 965.517 |
| IAPY base fumed | 1.058 | 539 | 0.5186 | 2.1016 | | | 0.9098 | 0.0908 | | | 0.5806 | 5.89 | 101.447 | 1620.909 |
| IAPY Hexane | 1.037 | 515 | 0.0559 | 0.5962 | | | 0.4907 | 0.5093 | | | 0.0556 | 20.22 | 3636.69 | 14348.92 |
| IAPY 1,4-dioxane | 1.069 | 518 | 0.0645 | 0.0634 | | | 0.4842 | 0.5157 | | | 0.064 | 17.73 | 2770.312 | 12854.688 |
| IAPY EtOAc | 1.023 | 522 | 0.0629 | 0.0625 | | | 0.4949 | 0.5051 | | | 0.063 | 14.54 | 2307.936 | 13565.079 |
| IAPY DCM | 1.071 | 514 | 3.177 | 0.064 | | | 0.0012 | 0.9988 | | | 0.068 | 13.33 | 1960.294 | 12745.588 |
| IAPY $CHCl_3$ | 1.006 | 521 | 2.9433 | 0.0759 | | | 0.0011 | 0.9988 | | | 0.079 | 12.79 | 1618.987 | 11039.241 |
| IAPY N,N-DMF | 1.019 | 526 | 0.0719 | 5.0988 | | | 0.9995 | 0.0005 | | | 0.074 | 9.79 | 1322.972 | 12190.5405 |

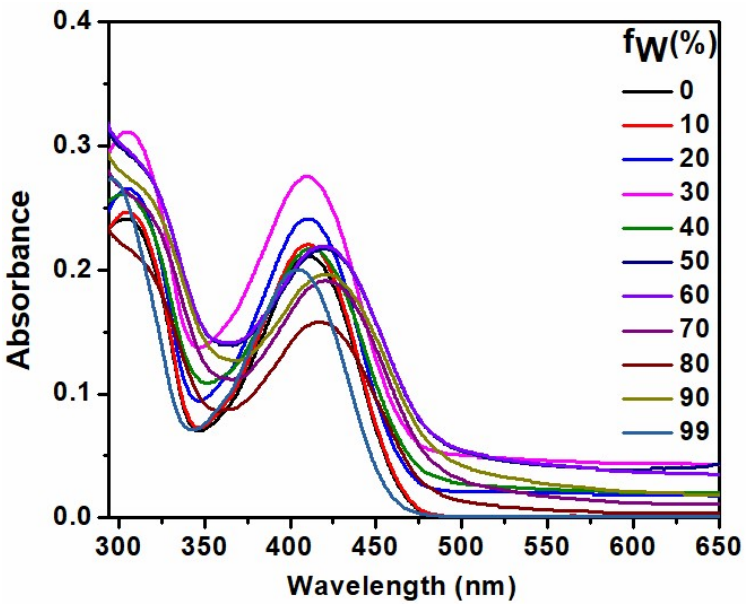


**Fig. S31** Absorbances for AIE-study of **IAPY**

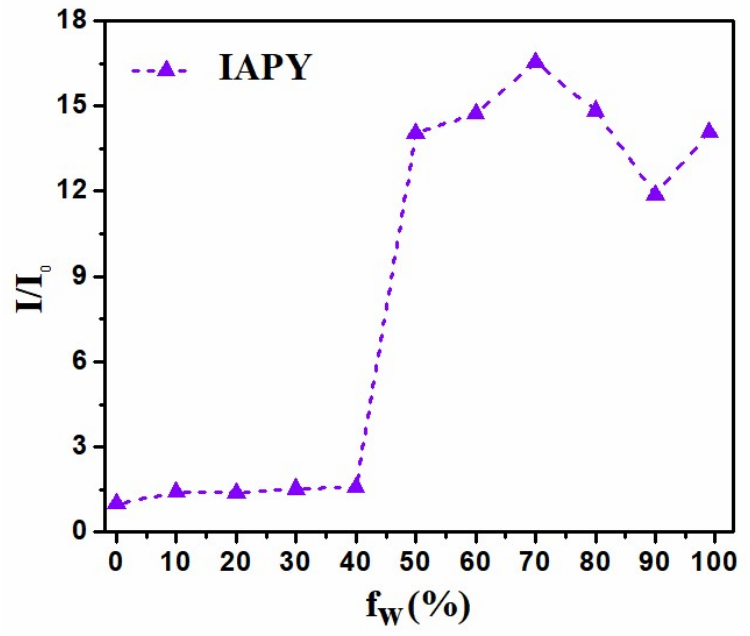


**Fig. S32** Intensity of emission increment for AIE at $10^{-5}$M concentration of **IAPY**

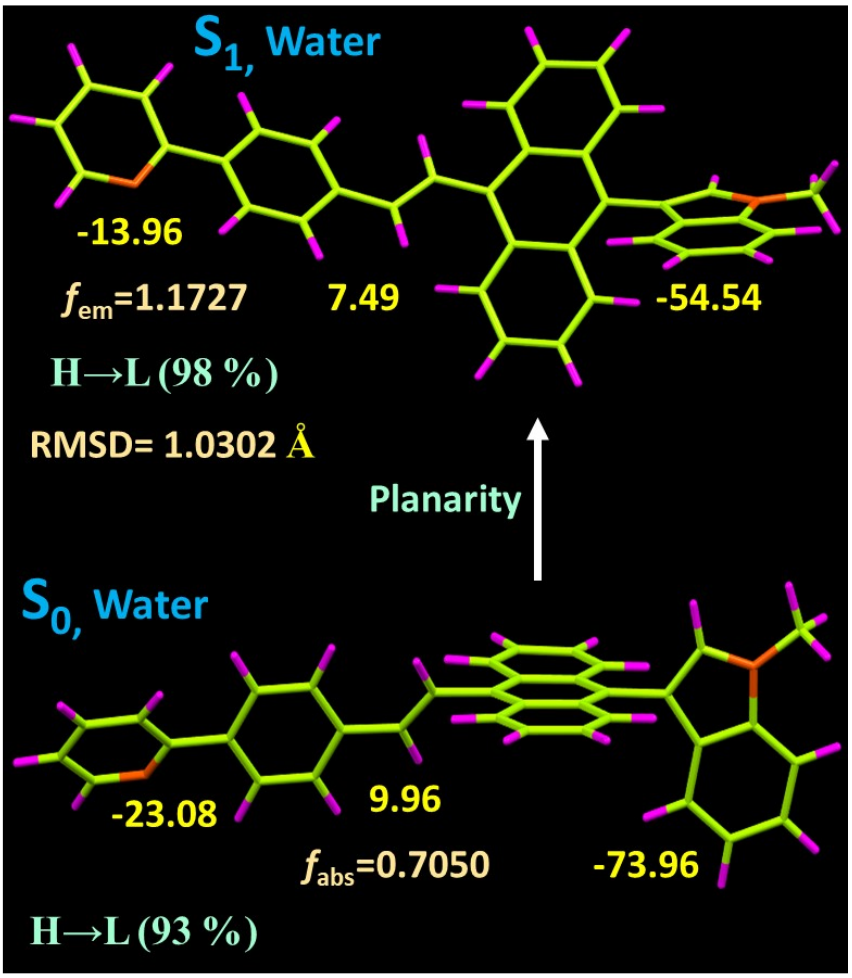


**Fig. S33** TD-DFT optimized structure of **IAPY** in water

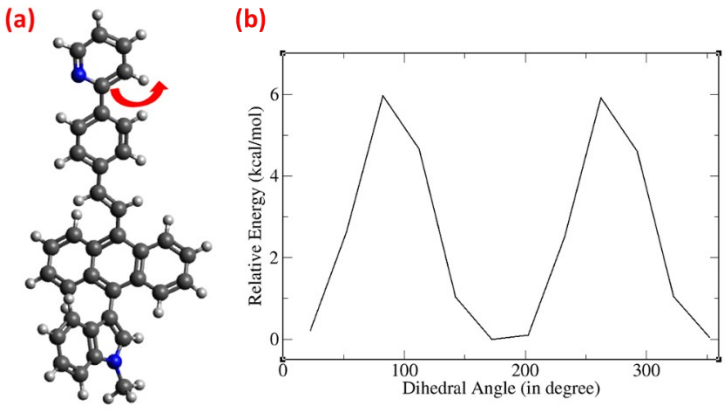


The rotation barrier is very small ~6 kcal/mol. That's free rotation takes place and excited state energy can decay non radiatively.

**Fig. S34a** Rotation barrier of the Pyridine group in $S_1$ state

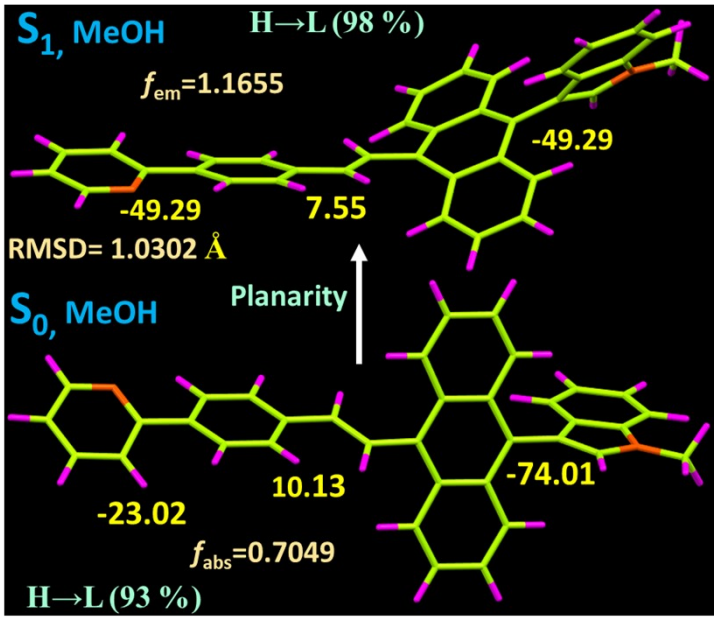


**Fig. S34b** TD-DFT optimized structure of **IAPY** in MeOH

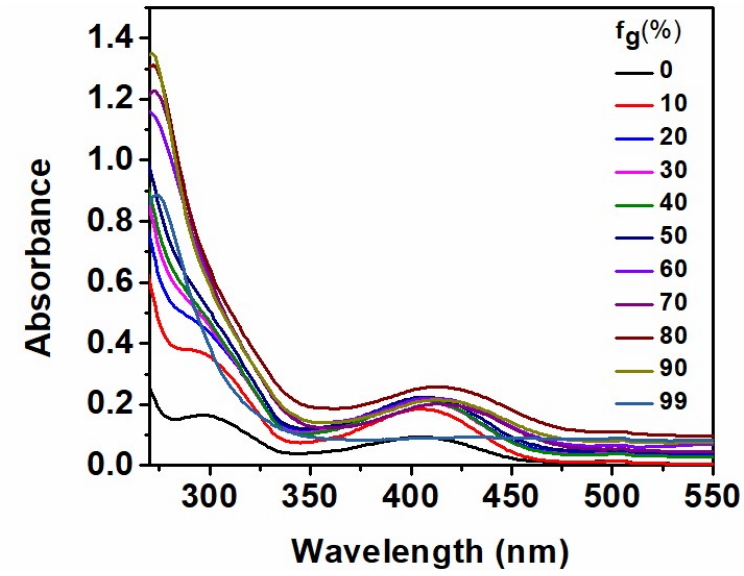


**Fig. S35** Absorbances for viscofluorochromism of **IAPY**

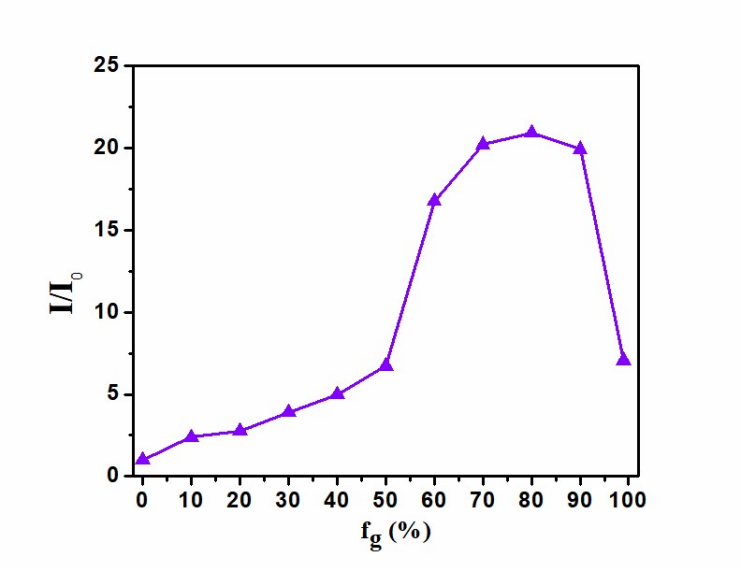


**Fig. S36** Intensity of emission increment for VIE at $10^{-5}$M concentration of **IAPY**

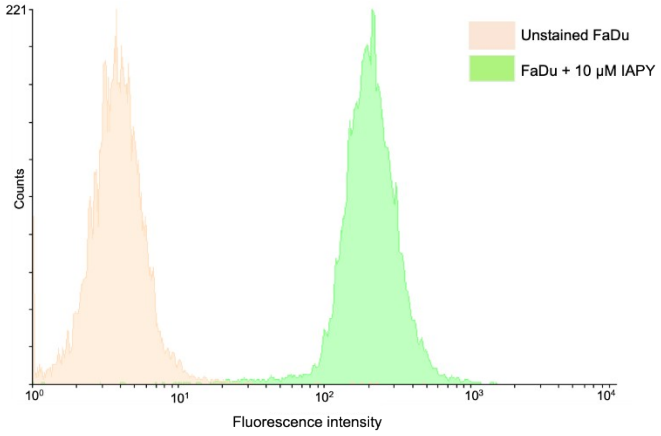


**Fig. S37** Cellular uptake of the probe **IAPY** through Fluorescence Activated Cell Sorting (FACS)

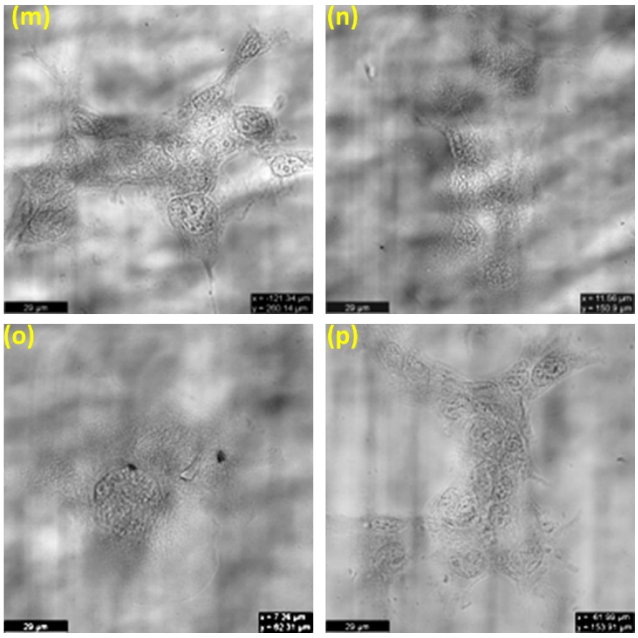


**Fig. S38** Bright field images for wash-free bioimaging of FaDu with **IAPY** (10 µM)

**Cell Culture and confocal microscopy**

The cell line was bought from ATCC and preserved in DMEM supplemented with 10% FBS with 1% (v/v) penicillin-streptomycin antibiotics. Cells were incubated at 37°C in a humidified atmosphere comprising 5% $CO_2$. All the culture supplies were procured from Thermo Fisher Scientific.

Cell line was seeded on a lysine-coated sterile coverslip placed on a 12-well cell culture plate ($1 \times 10^5$ cells per well) in DMEM containing 10% FBS with 1% antibiotics. Cells were allowed to adhere completely. After 24 h, cells were treated with formulation using 10µM probe concentration for 4 h. Later, cells were not washed with sterile PBS and mounted on a glass slide. Cell imaging was done using a confocal microscope (Leica LAS X).

**FACS**

FaDu cells were seeded in a 12-well plate at a density of 0.2 million cells per well. The cells were treated with IAPY at 10 µM concentration while the unstained control cells were treated with DMSO. After 24 hours of treatment, the medium was removed and cells were washed with PBS and trypsinized to obtain a single cell suspension. The cells in trypsin were centrifuged at 2000 rpm for 10 minutes at 4 degrees and resuspended in PBS for uptake analysis using BD FACS Aria II flow cytometer.

**Device fabrication, formulation with dye for screen printing and the procedure for screen printing**

A market-available screen-printing liquid (SPL) white non-fluorescent dye of 4000 cP was purchased. Later 30 mg of IAPY dye was dissolved in 10 ml of DMSO and sonicated unless the solution becomes clear. Now this solution was added with 30 ml of the screen-printing liquid white non-fluorescent dye and mixed properly to prepare an **IAPY-SPL** media. Again, by using another dye **SB6** the **SB6-SPL** media was prepared in the same fashion. The QR code was drawn with CAD tool solid works, and on the PVC sheet the QR code was engraved with the universal laser system $CO_2$ laser with 10-micron wavelength with 10% into 30 watts. The **SB6-SPL** was first painted on a glass surface and dried subsequently. The surface emiited green under 365-UV lamp. Later on, the laser-cut QR code pattern was screen printed

with **IAPY-SPL** on the surface of **SB6-SPL**. With naked eyes the QR-code is not clearly visible under ambient light. Even under 365-UV lamp also the entire surface remains green. Once the acid fumigation is done the QR-code will be visible under 365-UV lamp as it glows yellow on a green surface.

**Procedure and method of data storage and anticounterfeiting applications with stimuli-responsive hidden stamp:**

Three dyes- **IAPY**, **ATh4P**, and **SB6** were initially chosen as all of them are green emitters ($\lambda_{em.\ max}$= 501 nm-517 nm). An ethanolic solution of $10^{-7}$M concentration was prepared of each dye and soaked with three different sponges. Now a wooden stamp was pressed on the **IAPY** solution-soaked sponge and placed on a TLC plate to get an **IAPY** led stamp. Later on, the wooden stamp was washed with acetone properly, and consecutively, two more **ATh4P** and **SB6** led stamps were prepared on the TLC plates. Now, none of the stamps are visible to the naked eye but under the UV-365 nm lamp, all the stamps glow green. Now how to identify which stamp is real and which ones are counterfeited? Let us say that the **IAPY** is the real dye; hence, the **IAPY** led stamp will be the real stamp. **IAPY** emits orange-red on acid-fumigation but immediately does not revert back to green on base-fumigation as it turn yellow. But this information is secret. The counterfeiters might mimic a dye (**SB6**) which is a green emitter but not acidofluorochromic or can mimic a dye (**ATh4P**) which can emit red on acid fuming and again revert back to green on base fuming. Because reversible acidofluorochromism is usually used in most of the cases. So, if an unknown stamp that looks alike the real one, is acid-fumed and still emits green; it means the dye is counterfeited and the stamp is unreal. Next, if an unknown stamp that looks alike again as the real one, is acid-fumed and turns red emitting then that stamp may or may not be real. But again, with base-fuming if it turns green emitting instantly, then the stamp (made of dye **ATh4P**) is fake with no doubt. But on further base-fuming if it turns yellowish then the stamp is the real stamp.

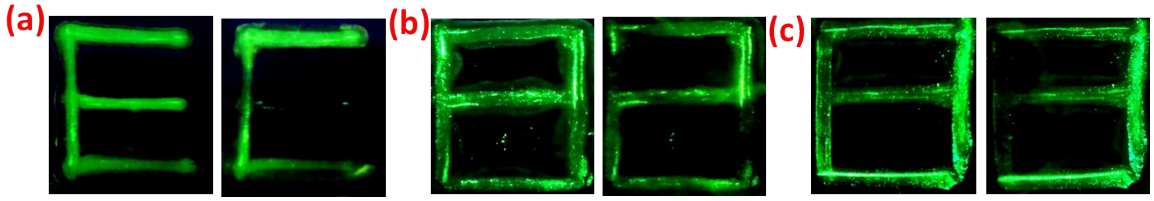


**Fig. S39** Data encryption with **IAPY**

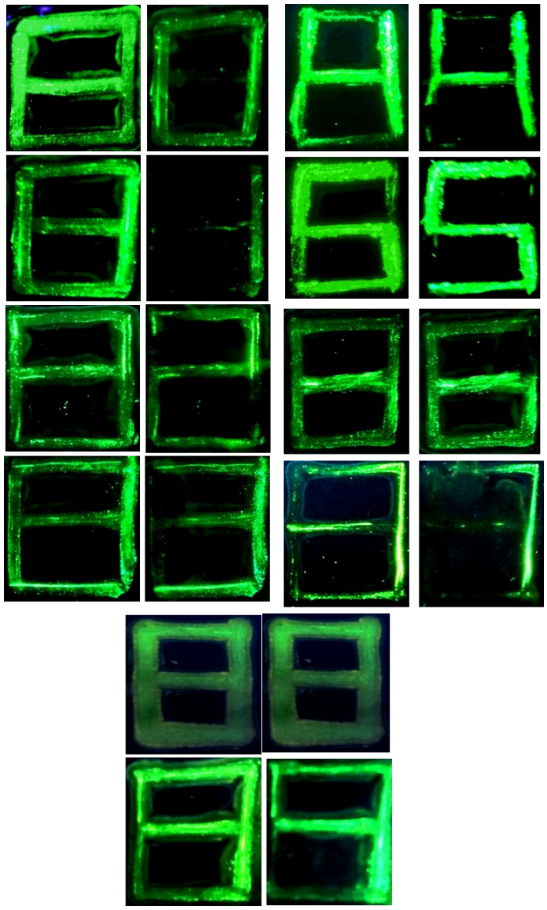

**Fig. S40** Data encryption with **IAPY** to make different digits from '8'

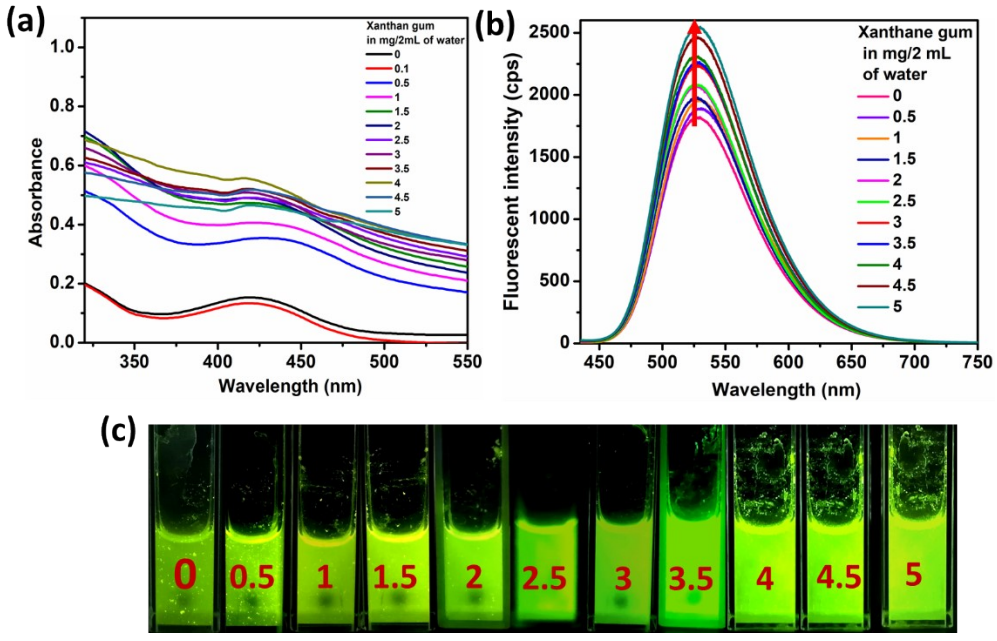


**Fig. S41** Xanthan gum sensing (a) absorbances (b) emission (c) picture taken under UV-365 nm lamp (the mg of Xanthan gum taken per 2ml of water is written on each cuvette picture)

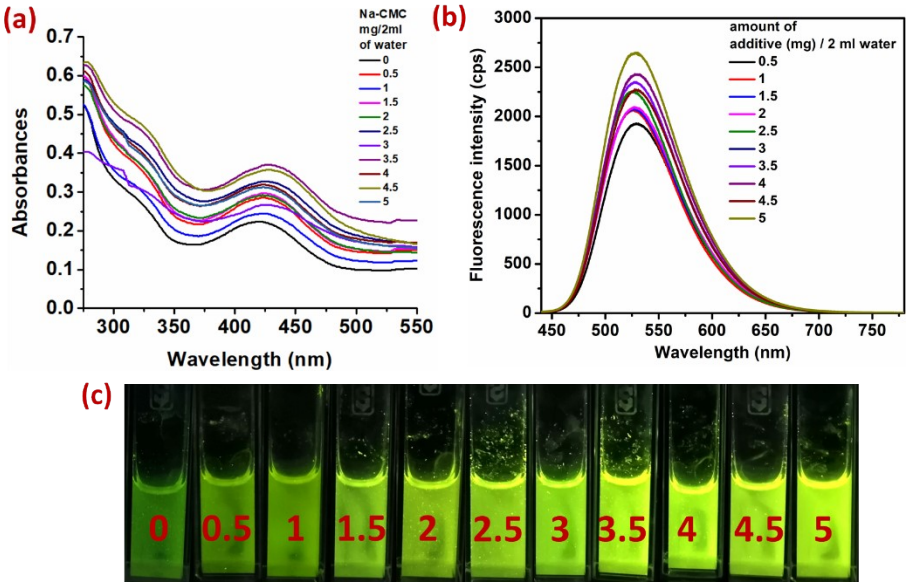


**Fig. S42** Na-CMC sensing (a) absorbances (b) emission (c) picture taken under UV-365 nm lamp (the mg of Na-CMC taken per 2ml of water is written on each cuvette picture)

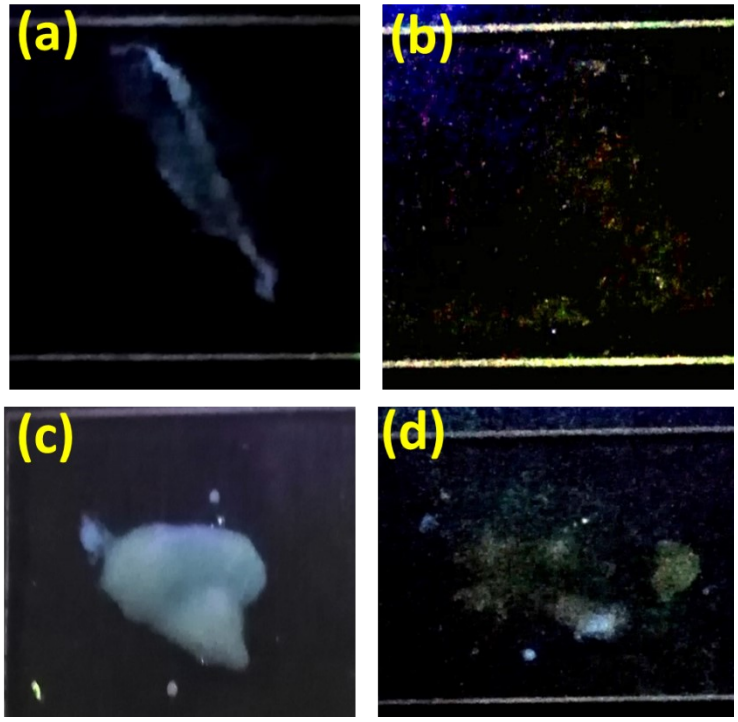


**Fig. S43** False-positive taste under UV-365 nm lamp; (a) dried patches of cold drinks (b) almost no fluorescence after staining with **IAPY** (c) tomato sauce (d) feeble green fluorescence after staining with **IAPY.**

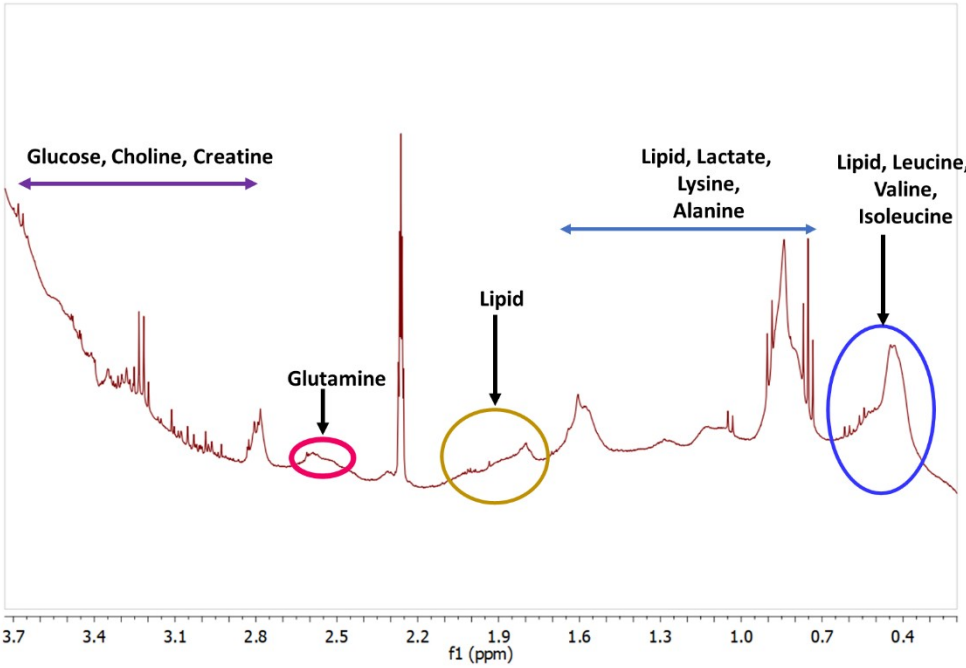


**Fig. S44a** Blood serum NMR

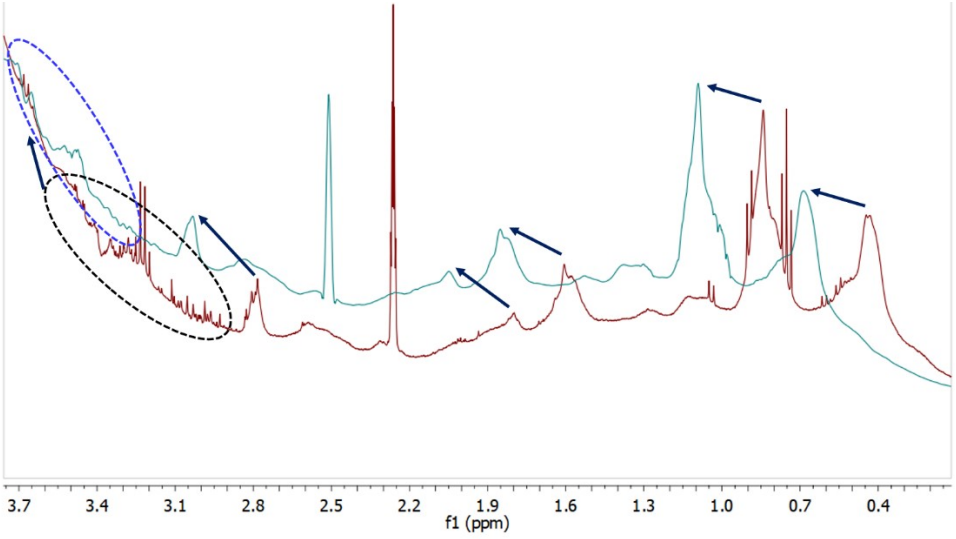


**Fig. S44b** Blood serum-NMR comparison (the maroon color line for **normal serum** and the sea-green color line for (**IAPY+serum**). The peaks for (**IAPY+serum**) are de-shielded from that of **normal serum.**

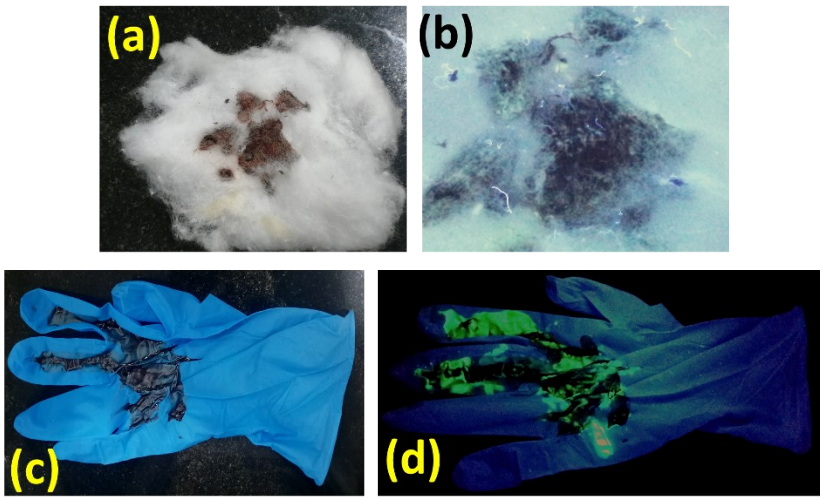


**Fig. S45** Hospital-disposed of biohazards detection by fluorescence; under normal room light (a) blood-smeared cotton (c) blood containing glove; under UV-365 nm lamp (b) blood-smeared cotton (d) blood containing glove

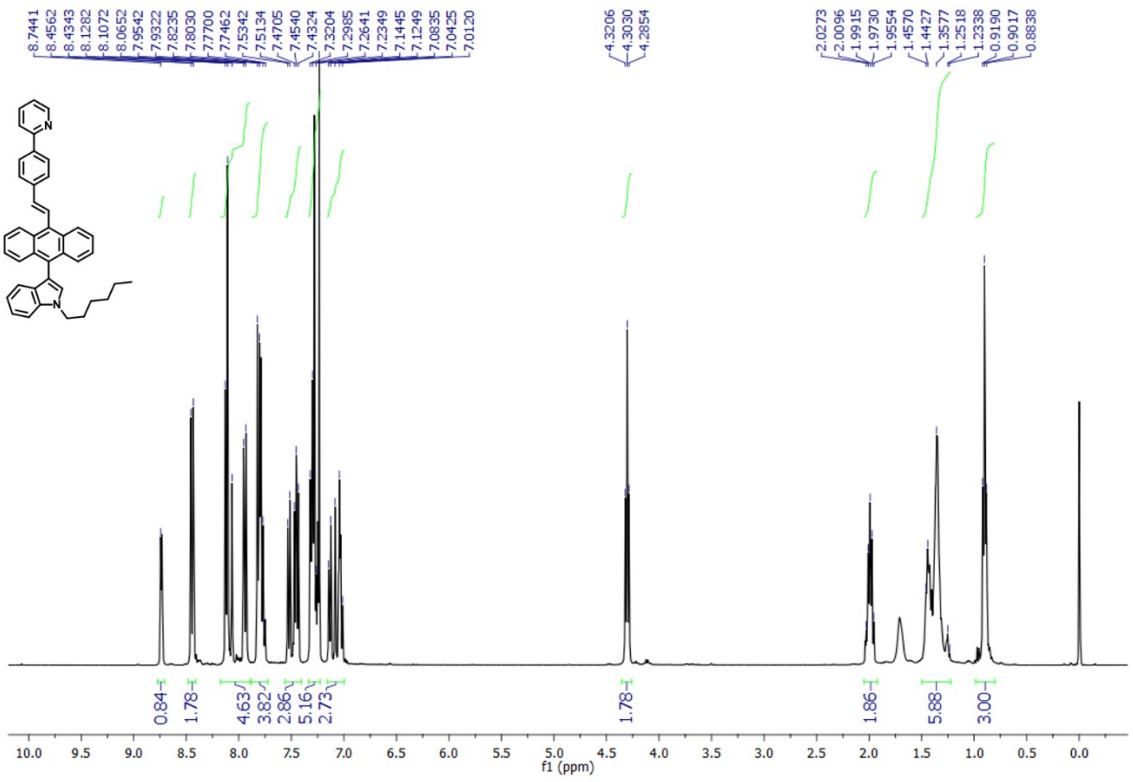


**Fig. S46** $^{1}$H NMR of **IAPY**[1]

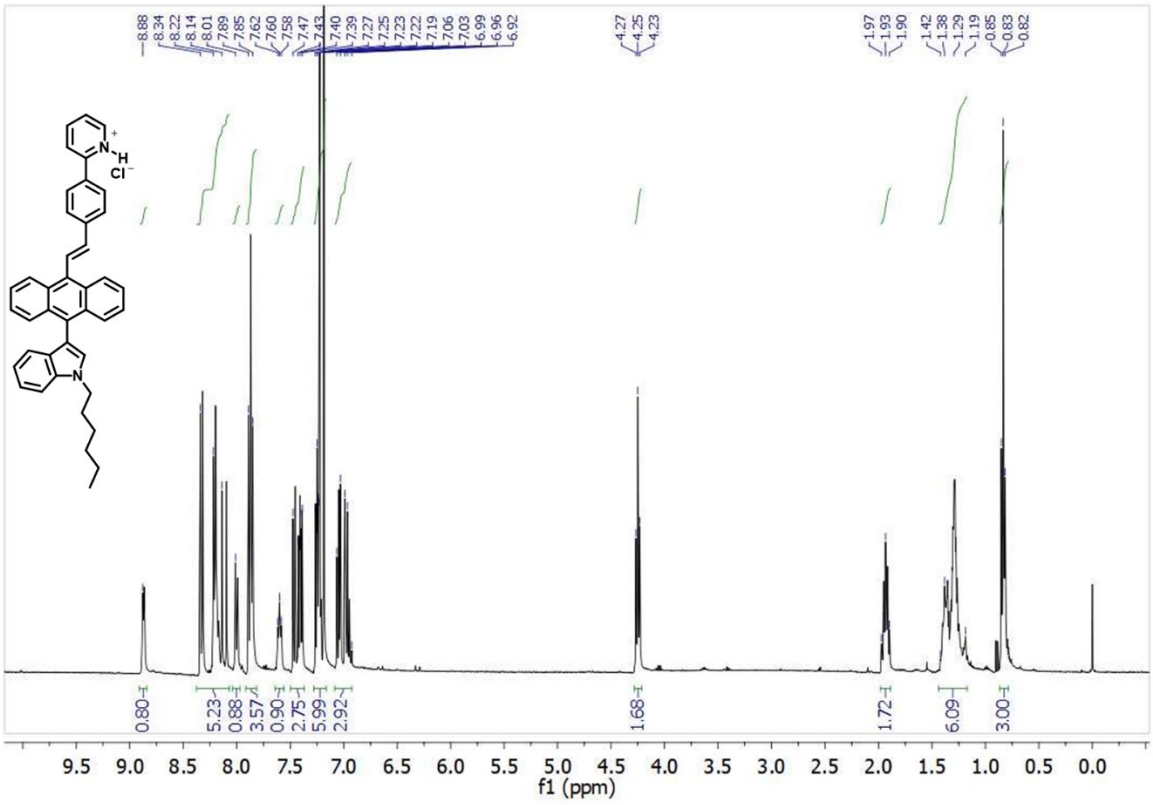


**Fig. S47** $^{1}$H NMR of **IAPYH**

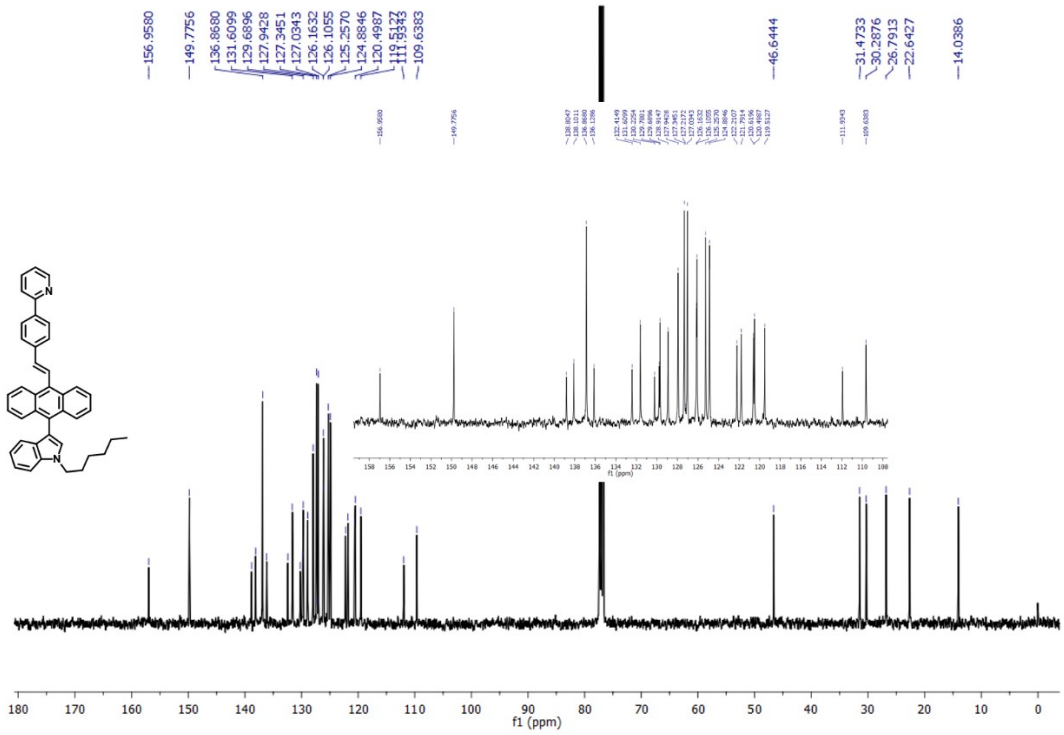


**Fig. S48** $^{13}$C NMR of **IAPY**[1]

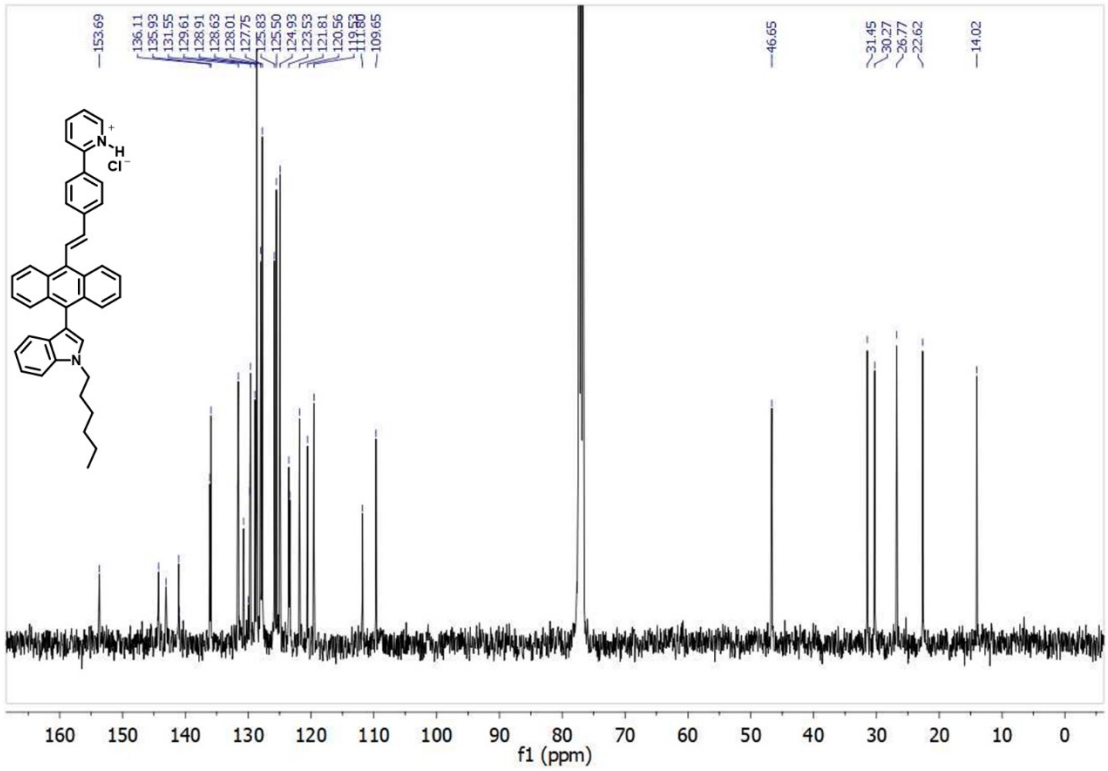


**Fig. S49a** $^{13}$C NMR of **IAPYH**

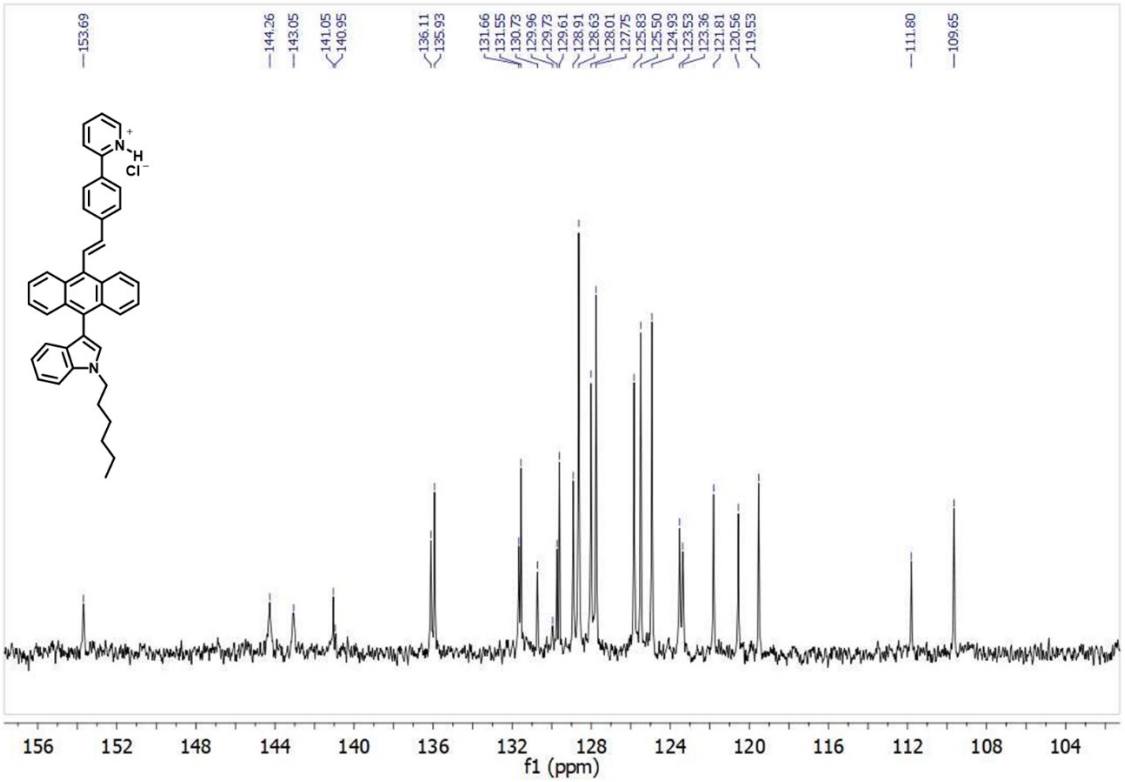


**Fig. S49b** $^{13}$C NMR (aromatic part zoomed) of **IAPYH**

## References

1 S. Bhuin, P. Sharma, P. Chakraborty, O. P. Kulkarni and M. Chakravarty, *J. Mater. Chem. B*, 2023, **11**, 188-203.

2 R. Rotaru, M. Savin, N. Tudorachi, C. Peptu, P. Samoila, L. Sacarescu and V. Harabagiu, *Polym. Chem.I*, 2018, **9**, 860-868.

3 F. Neese, F. Wennmohs, U. Becker and C. Riplinger, "The ORCA Quantum Chemistry Program Package", *Journal of Chemical Physics*, 2020, **152**, 224108.

4 F. Neese, "Software Update: The ORCA Program System-Version 5.0." *WIREs Computational Molecular Science*, 2022, **2**, 73-78.

5 T. Yanai, D. Tew, and N. Handy, "A new hybrid exchange-correlation functional using the Coulomb-attenuating method (CAM-B3LYP)," *Chem. Phys. Lett.I*, 2004, **393**, 51-57.

6 W. Kabsch, A solution for the best rotation to relate two sets of vectors, *Acta Crystallogr.*, 1976, **A32**, 922-923. (Code: https://github.com/charnley/rmsd)

7 Hanwell, D. Marcus et al. "Avogadro: an advanced semantic chemical editor, visualization, and analysis platform", *J. Cheminformatics*, 2012, **4**, 1-17.

END